Biochemistry and Biophysics Reports 4 (2015) 59–75

Contents lists available at ScienceDirect

Biochemistry and Biophysics Reports

journal homepage: www.elsevier.com/locate/bbrep

Enzymatic attributes of an L-isoaspartyl methyltransferase from *Candida utilis* and its role in cell survival

Shakri Banerjee [a], Trina Dutta [a], Sagar Lahiri [a], Shinjinee Sengupta [a], Anushila Gangopadhyay [b], Suresh Kumar Karri [b], Sandeep Chakraborty [b], Debasish Bhattacharya [c], Anil K. Ghosh [a,*]

[a] Drug Development, Diagnostics and Biotechnology Division, CSIR-Indian Institute of Chemical Biology, 4, Raja S.C. Mullick Road, Kolkata 700032, India
[b] Infectious Diseases and Immunology Division, CSIR-Indian Institute of Chemical Biology, 4, Raja S.C. Mullick Road, Kolkata 700032, India
[c] Structural Biology and Bioinformatics Division, CSIR- Indian Institute of Chemical Biology, 4, Raja S.C. Mullick Road, Kolkata 700032, India

ARTICLE INFO

Article history:
Received 2 June 2015
Received in revised form
23 August 2015
Accepted 24 August 2015
Available online 28 August 2015

Keywords:
Isoaspartate
Deamidation
Enzyme catalysis
Enzyme purification
Yeast
S-adenosyl l-methionine
MALDI TOF

ABSTRACT

Backgrounds: Spontaneous deamidation and isoaspartate (IsoAsp) formation contributes to aging and reduced longevity in cells. A protein-L-isoaspartate (D-aspartate) O-methyltransferase (PCMT) is responsible for minimizing IsoAsp moieties in most organisms.
Methods: PCMT was purified in its native form from yeast *Candida utilis*. The role of the native PCMT in cell survival and protein repair was investigated by manipulating intracellular PCMT levels with Oxidized Adenosine (AdOx) and Lithium Chloride (LiCl). Proteomic Identification of possible cellular targets was carried out using 2-dimensional gel electrophoresis, followed by on-Blot methylation and mass spectrometric analysis.
Results: The 25.4 kDa native PCMT from *C. utilis* was found to have a K_m of 3.5 μM for AdoMet and 33.36 μM for IsoAsp containing Delta Sleep Inducing Peptide (DSIP) at pH 7.0. Native PCMT comprises of 232 amino acids which is coded by a 698 bp long nucleotide sequence. Phylogenetic comparison revealed the PCMT to be related more closely with the prokaryotic homologs. Increase in PCMT levels *in vivo* correlated with increased cell survival under physiological stresses. PCMT expression was seen to be linked with increased intracellular reactive oxygen species (ROS) concentration. Proteomic identification of possible cellular substrates revealed that PCMT interacts with proteins mainly involved with cellular housekeeping. PCMT effected both functional and structural repair in aged proteins *in vitro*.
General significance: Identification of PCMT in unicellular eukaryotes like *C. utilis* promises to make investigations into its control machinery easier owing to the familiarity and flexibility of the system.

1. Introduction

Cellular proteins go through spontaneous, non-enzymatic modifications like deamidation of specific asparagines or dehydration of aspartyl residues and give rise to unusual β-linked L-isoaspartyl residues (Fig. 1) [1,2]. Generation of these isoAsp residues introduces a kink in the protein backbone that may threaten to alter the functionally active structure of a protein (Fig. 1) [2]. Deamidation at asparaginyl sites and subsequent formation of isoaspartyl residues in their places poses to be potentially disruptive to protein function coupled with an increased tendency to aggregate [3]. The abnormal isoAsp residues are recognized by an enzyme, protein-L-isoaspartate (D-aspartate) O-methyltransferase or PCMT (EC 2.1.1.77). PCMT selectively methylates the α-carboxyl sidechain of L-isoaspartyl and/or naturally occurring D-aspartyl residues by transferring the methyl group from S-adenosyl L-methionine (AdoMet) and initiates the restoration of these abnormal residues back to normal amino acids (Fig. 1) [4]. The L-isoaspartyl/D-aspartyl methyl esters release one molecule of methanol to form an L-succinimide intermediate. The L-succinimide intermediate undergoes structural rearrangement and hydrolyzes into either normal L-aspartyl (30%) or abnormal L-isoaspartyl (70%), depending on the bond broken. The L-succinimide may spontaneously racemize into D-succinimide which hydrolyzes to produce a mixture of D-aspartyl and D-isoaspartyl residues. These abnormal residues then again undergo another methylation cycle by PCMT (Fig. 1) [5]. Multiple cycles of this process brings about either complete (Asp to Asp via IsoAsp) or partial (Asn to Asp via IsoAsp) repair of the age-damaged protein [6]. The success of this protein repair mechanism lies in the fact that it restores the correct conformation of the protein backbone [4]. *In vitro*, this process repairs

* Corresponding author. Fax: +91 33 2473 5197.
E-mail addresses: anilghosh51@gmail.com, aghosh@iicb.res.in (A.K. Ghosh).

http://dx.doi.org/10.1016/j.bbrep.2015.08.015

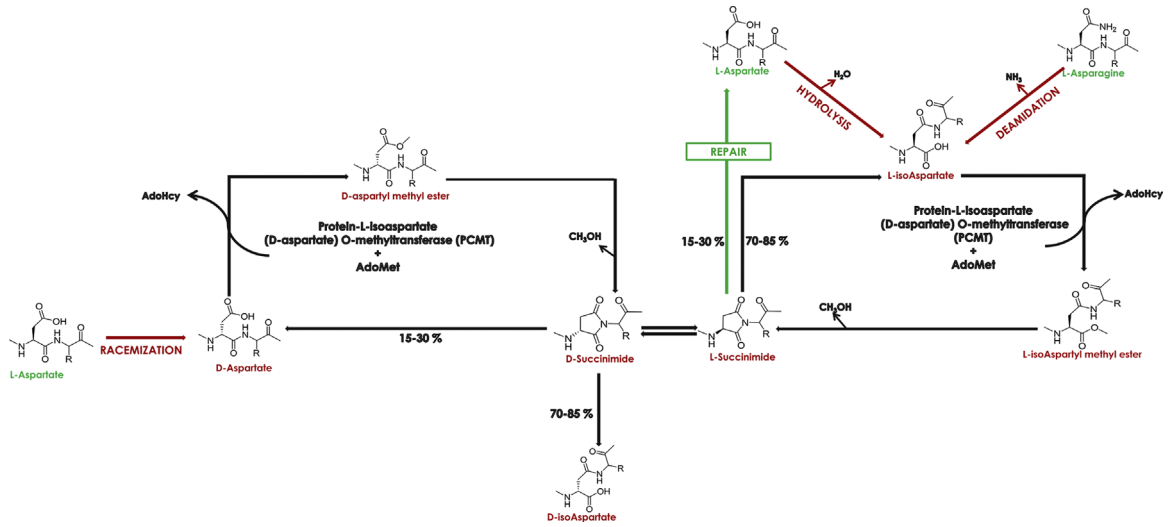

Fig. 1. Mechanism of isoAsp repair by Protein Carboxyl Methyltransferase (PCMT)**.** During prolonged storage at physiological pH, native proteins or peptides undergo either deamidation at L-asparaginyl residues or isomerisation and racemisation at L-aspartyl residues, resulting in the formation of abnormally linked L-isoaspapartates or D-aspartates. These damaged proteins or peptides exhibit reduced cellular functions. Protein L-isoaspartate (D-aspartate) O-methyltransferase (PCMT) targets these L-isoAsp or D-aspartate residues to catalyze their selective methylation with the aid of methyl group donor S-adenosyl L-methionine (AdoMet). The methylation step leads to the formation of L-isoaspartyl or D-aspartyl methyl esters along with a molecule of S-adenosyl L-homocysteine (AdoHcy). A metastable succinimide intermediate is produced when the methyl esters lose a molecule of methanol (CH_3OH) spontaneously. The L-succinimide intermediate hydrolyzes to generate a mixture of L-isoaspartyl and L-aspartyl residues, or it spontaneously gets racemized into D-succinimide which upon hydrolysis results into a mixture of D-isoaspartyl and D-aspartyl residues. Each methylation cycle reduces the total L-isoaspartate (and D-aspartate) level in a protein or peptide population by 15–30% relative to the previous cycle, resulting in a net repair of $\geq$ 85% after 10 or more cycles. The active amino acid residues and the step leading from inactive abnormally linked residue to its active form are marked in green. The inactive residues and the steps leading to formation of an abnormally linked form of amino acid are marked in red.

IsoAsp containing peptides and restores activity by 50% in structural as well as enzyme proteins [7].

Repair is the energetically efficient option for rescuing aged proteins rather than resorting to the hugely energy expensive process of protein recycling [6]. The importance of this protein repair mechanism and the enzyme PCMT is underlined by its wide distribution and its high degree of sequence conservation among varied life forms [8]. PCMT is found in most bacteria [9], plant [10], nematodes [11], flies [12], and mammals including humans [13]. Survival and longevity of certain bacteria, nematodes and mammals have been shown to be dependent on PCMT levels and was seen to be significantly reduced when deficient [14–16].

PCMT research has seen tremendous boost in the last decade. Research has focused on its physiological role in protein repair and cell survival. PCMT has been identified and isolated from higher plants, animals, but reports in fungi have not yet seen much endeavor. Owing to fast next generation sequencing techniques, a large portion of the yeast genomes have been sequenced. In most of these, the PCMT gene has been predicted but little efforts have been directed towards their isolation and characterization. Sequencing and subsequent annotation revealed that the genome of *Saccharomyces cerevisiae* lacked a PCMT gene or its homolog [17,18]. In contrast, a PCMT homolog, Pcm2, has been identified in fission yeast *Schizosaccharomyces pombe* [19]. Unicellular fungi or yeasts have been used as crucial tools in elucidating the key components of biological processes like cell cycle and apoptosis. A similar approach may work for PCMT in elucidating its regulatory mechanisms as well as downstream substrates thus underlining its role in physiological processes.

Till date, to the best of our knowledge, no published report elucidates purification of a native PCMT enzyme from any unicellular fungi or yeast. The present work is directed towards identifying and purifying a native PCMT activity in the unicellular fungi *C. utilis*. The sequence of the purified PCMT was worked out. An in depth study on the repair ability of the purified enzyme was performed with common cellular proteins, catalytic and structural, subjected to aging under physiological conditions. Role of PCMT activity was demonstrated *in vivo* in relation with cell survival under stress and cellular targets of the PCMT were identified employing 2D gel electrophoresis followed by mass spectrometric analyses. In short, our study reports the first isolation of a PCMT enzyme from yeasts in its native form along with a study of its repair activity and contributes important information to the knowledgebase of PCMT in *C. utilis*.

2. Materials and methods

2.1. Materials

Media components and agar powder were purchased from Himedia, India. Solvents of HPLC grade were procured from Merck, Germany. All chemicals were purchased from Sigma Aldrich, USA. S-Adenosyl-(methyl-^{3}H)-L-Methionine was purchased from Perkin-Elmer, USA. ISOQUANT® Isoaspartate Detection Kit and Sequencing grade Modified Trypsin was obtained from Promega, USA. All the other chemicals and media components were of analytical grade and purchased locally.

2.2. Organism and culture conditions

The wild type *C. utilis* strain was obtained from National Chemical Laboratories, Pune, India (Cat. No. NCIM Y500). Cells were grown in YPD (Yeast Extract–5%, Peptone–1% and D-glucose–2%) medium at 30 °C with mechanical shaking at 200 rpm unless otherwise mentioned [20].

A Δ*pcmt* strain of *C. utilis* was generated for the purpose of this study. The gene was disrupted using a yeast plasmid pFA6a-kanMX6 as the template for a PCR reaction [21]. Primers used for the PCR amplification reaction of the selectable marker gene (*E. coli* kanamycin resistance gene *kan*^{r}) are; forward primer-5′

ATGGCTCAATTTATTAATCATTTGTTTTGGTCATTTAATTCGGATCCCC-GGGTTAATTAA 3′ and reverse primer 5′GGATACCAAACAGTTTGA-GCCAATTGTGATGGATCTTTACGAATTCGAGCTCGTTTAAAC 3′. The PCR product was transformed into the *C. utilis* cells using a reported protocol [22]. Disruption of the TPP gene was facilitated by homologous recombination. The wild-type *C. utilis* cells were sensitive to antibiotic G418/geneticin and the mutants (Δ*pcmt*) were selected by growing in YPD plates supplemented with 200 mg/ml G418. For experiments Δ*pcmt C. utilis* cells were grown in liquid YPD media supplemented with 200 mg/ml G418 under mechanical shaking at 200 rpm.

2.3. Methods

2.3.1. Preparation of cell free extract

C. utilis cells were grown in YPD medium up to appropriate growth phase monitored by measuring the turbidity of the culture at 660 nm. Cell suspension (3 ml) were harvested by centrifugation at 500*g* for 5 min and washed twice with sterile triple distilled water. Pellet was dissolved in 0.3 ml of ice cold lysis buffer (50 mM Na-Phosphate buffer, pH 7.0, 10% (w/v) glycerol, 0.1% (v/v) TWEEN-40, 1 mM PMSF, 2 mM Benz-HCl and 10 μl Protease Inhibitor cocktail from Sigma) and were lysed by mechanical disruption with 36 mg acid washed glass beads (size 425–600 μm, Sigma, USA). Cells were disrupted by 6 rounds of vortexing for 60 s with 90 s rests on ice in between to prevent heating. The lysate was centrifuged for 15 min at 3000*g* to remove unlysed cells and other debris. The supernatant was collected and stored at −20 °C until analysis. The protein contents of semi-purified and purified enzyme solutions were determined by the Lowry protein assay [23]. Protein content of whole cell homogenate was measured by the modified method of Lowry [24].

2.3.2. Measurement of isoaspartyl content

Isoaspartate content was measured with the ISOQUANT Isoaspartate Detection Kit from Promega, USA. The reaction had a final reaction volume of 50 μl. Concentration of the reference isoAsp DSIP solution used in the assay was 1 μM. Cell lysate incorporated in the assay was 50 μg whereas protein samples were incorporated at a concentration of 20 pmoles. The reaction was carried out following the manufacturer's directions for the radioactive detection protocol. Isoaspartate concentration was expressed either as pmoles isoAsp/mg total proteins (for cell lysates) or as pmoles isoAsp/pmol protein (for individual proteins).

2.3.3. Determining the nature of isoaspartyl protein removal in C. utilis

50 ml YPD media was inoculated with 500 μl overnight cultures of *C. utilis* and incubated at 30 °C until the cultures reached early stationary phase or A_{660}∼23. Cells were harvested at 500*g*, washed twice with PBS and resuspended in fresh 50 ml YPD media containing AdOx (1 mM), MG132 (30 μM) or 3-methyladenine (5 mM). The cultures were incubated for 24 h at 30 °C. After incubation cells were harvested as previously mentioned. Cell pellets were lysed (0.1 g) with glass beads as mentioned earlier and Isoaspartate levels were determined.

To determine whether cellular proteases play role in degrading isoaspartate containing proteins, Δ*pcmt C. utilis* cells were grown upto early stationary phase (A_{660}∼23), cells were harvested and lysed with glass beads as mentioned earlier. The cell free extract was brought to a concentration of 3 μg/μl by adding *in vitro* aging buffer (20 mM Tris–HCl, pH 7.5, 20 mM NaCl, 1 mM EDTA, 2% (v/v) glycerol, 0.05% (w/v) NaN_3) with the following additives in separate sets: (i) 5 mM EDTA, pH 8.0 (ii) 40 μM Pepstatin A, (iii) 1 mM PMSF, (iv) 25 μM Leupeptin or (v) 50 mM NaCl serving as control. Cells were incubated at 37 °C for 72 h. At the end of incubation, each set was measured for isoaspartate levels.

2.3.4. Isoaspartyl methyltransferase enzyme assay

PCMT activity was assayed after a published protocol with certain modifications [6]. Assay mixture volume was 300 μl with 0.05 M phosphate–citrate–EDTA buffer, pH 6.8 and 40 μM (methyl-^{3}H) AdoMet (specific activity: 15 mCi/mM) with incubation at 30 °C. PCMT enzyme incorporated in the assay varied between 0.01 and 0.14 ml (300 μg in case of crude extracts and 6 μg of purified enzyme). IsoAsp DSIP was used as the substrate for all steps of purification in a concentration 350 μM unless otherwise mentioned. Reaction was stopped with the addition of 300 μl 0.45 M sodium borate (pH 9.6) containing 4% (w/v) SDS and 2% (v/v) Methanol. The base labile (^{3}H) methanol formed was detected after 18–24 h of incubation in the scintillation Cocktail O by a liquid scintillation counter (Perkin-Elmer). Unit of enzyme activity (U) was defined as pmoles of methyl groups transferred per minute and specific activity of the enzyme was defined as U/mg protein.

2.3.5. Enzyme assays

2.3.5.1. Hexokinase (Hx) enzyme assay. Hexokinase (Hx) was assayed following protocol published by Magnani et al. [25]. Total volume of reaction mixture was 2.57 ml containing 39 mM triethanolamine buffer, pH 7.6, 216 mM D-glucose, 0.74 mM β-$NADP^+$, 7.8 mM $MgCl_2$ and 2.5 Units of glucose-6-phosphate dehydrogenase. Hx activity was measured spectrophotometrically by noting the increase in absorbance at 340 nm. Unit Hx enzyme activity was defined as μmoles of glucose-6-phosphate produced per minute at 30 °C.

2.3.5.2. Glutamate dehydrogenase (GDH) enzyme assay. Glutamate dehydrogenase (GDH) activity was assayed by the oxidation reaction [26]. Assay solution (0.9 ml) contained 25 mM glutamate, 50 mM Tris (pH 9.5), 2.5 mM EDTA, 1.4 mM NAD and 1 mM ADP. The change in absorbance was monitored at 340 nm. Unit GDH activity was defined as μmoles of NAD+ reduced per minute at 30 °C.

2.3.6. Purification of native PCMT activity from C. utilis

2.3.6.1. Cell lysis. 4 l cultures of *Candida utilis* were grown upto A660∼25 and 32 g cells were harvested by centrifugation at 500 × g for 5 min. The cell pellet was washed twice with ice cold, sterile, triple distilled water and finally re-suspended in lysis buffer. Lysis was achieved by passing cell suspension through FRENCH® Pressure Cell Press (SLM Instruments, USA) at 18,000 psi twice. The crude lysate was then centrifuged at 10,000*g* for 10 min, 4 °C. The pellet was discarded and the supernatant was dialyzed overnight against Dialysis Buffer (50 mM Na-Phosphate buffer, pH 7.0 containing 0.1 mM PMSF, 0.1 mM benzamidine hydrochloride, 0.5% (w/v) glycerol and 0.1% (v/v) TWEEN-40).

2.3.6.2. Protein precipitation. The dialyzed extract was subjected to stepwise ammonium sulfate fractionation and each fraction was checked for PCMT activity. Pellets obtained after each step was resuspended in minimum amount of Chromatography Buffer (Dialysis Buffer containing 150 mM NaCl).

2.3.6.3. High performance liquid chromatography. Ammonium sulphate fraction with maximum enzyme activity was injected to a High Performance Size Exclusion liquid chromatography (HPSELC) column, BioSuite SEC, 125 A°, 10 μm, 7.5 mm × 300 mm (Waters, USA). Chromatography Buffer was used as the mobile phase with a flow rate of 0.5 ml/min. The absorbance at 280 nm (A_{280}) was monitored along with peak quantification using Empower 2 Software (Waters, USA). Active fractions were pooled and

concentrated by Amicon™ Ultra device with molecular weight cut-off 10 kDa (Millipore, USA). The concentrated fraction was injected into a second HPSELC column Protein-Pak 125, 10 μm, 7.8 mm × 300 mm (Waters, USA). Same buffer and flow rate was applied. Active fractions were collected, concentrated as mentioned above, aliquoted, stored at −20 °C until further use and was designated as CuPCMT.

2.3.7. Purification validation

The desalted CuPCMT was injected into a high performance reverse phase liquid chromatography (HPRPLC) column, Deltapak C4, 300 A°, 3.9 mm × 300 mm (Waters, USA) for checking the purity of the enzyme preparation and eluted using a linear gradient of Solvent A (Water containing 0.1% TFA) and solvent B (Acetonitrile containing 0.1% TFA). Flow rate was maintained at 0.8 ml/min. A_{280} was monitored as stated earlier.

Homogenity was also validated by reinjecting the Step 4 enzyme mentioned in the preceding section into the Protein-Pak 125 column with same chromatographic conditions, buffers and flow rate.

2.3.8. Molecular weight determination of the native CuPCMT

The approximate molecular weight of the purified CuPCMT was estimated by HPSELC in Protein-Pak 125 as well as from SDS–PAGE. The chromatographic conditions, buffers and flow rate were same as mentioned earlier. SDS–PAGE was carried out following Laemelli [27], in a 12.5% resolving gel using discontinuous buffer system under constant current (20 mA/slab).

To determine the exact molecular weight of CuPCMT, 0.45 μl of the desalted enzyme was spotted onto α-cyano-4-hydroxy-cinnamic acid matrix and Matrix-assisted laser desorption–ionization time-of-flight mass spectrometry (MALDI TOF MS) analysis was performed using an Applied Biosystems Q10 4800 MALDI TOF/TOF™ analyzer. The 4000 series explorer software was used for data acquisition and GPS explorer software, version 3.6 for analysis.

2.3.9. Determination of secondary structure of the native CuPCMT

Secondary structure of the CuPCMT was worked out by circular dichroism (CD) analysis in a Jasco J715 spectropolarimeter (Japan Spectroscopic Ltd., Japan) having a scan speed 50 nm/min. Protein concentration used for both were 10 μM in 0.1 M potassium phosphate buffer (pH 7.5) and the spectra was recorded at a range of 200–260 nm. The cuvette used is of 1 mm pathlength. The spectra were reported in terms of mean residue molar ellipticity (θ) (deg cm^2 dmol^{-1}). Deconvolution of the CD spectra was done using the CDNN software [28].

2.3.10. Biophysical and biochemical characteristics of CuPCMT

2.3.10.1. Temperature and pH conditions. The optimum temperature as well as temperature stability for CuPCMT activity was evaluated by assaying the enzyme at different temperatures (10–90 °C) at pH 7.0. Optimum pH and pH stability for the CuPCMT was determined by measuring enzyme activities at 30 °C at pH ranging from 5.0 to 9.5 using the following buffer systems: 0.05 M sodium acetate (pH 5.0–6.0), 0.05 M sodium phosphate buffer (pH 6.5–7.5) and 0.05 M Tris–HCl (pH 7.5–9.5). The amount of protein in each assay set was 6 μg.

2.3.10.2. Substrate specificity assays. Substrate specificity of PCMT was checked for peptide and proteins substrates – isoaspartate containing Delta Sleep Inducing Peptide (IsoAsp DSIP), Ovalbumin, γ-globulin, and BSA. Aging of the BSA was carried out in the *in vitro* aging buffer for 10 days. The aged BSA was used as a substrate. The concentrations of all the substrates in the reaction were 0.2 mM. Amount of enzyme protein in the reaction was 6 μg.

2.3.10.3. Michaelis–Menten kinetic parameters. Michaelis–Menten kinetic parameters for CuPCMT were determined from the substrate saturation assays for the methyl group donor AdoMet as well as peptide substrate (isoAsp DSIP). Values for maximum velocity (V_{max}), half-saturation coefficient (K_m) and enzyme turn over number (K_{cat}) were determined from Michaelis–Menten plots [29]. Effect of methylation inhibitor, S-Adenosyl-L-homocysteine (AdoHcy), was studied using varying concentrations as 0, 0.2, 0.5, 0.8 and 1 mM. Inhibitory constant (K*i*) was determined graphically following Dixon [30].

2.3.11. Protein sequencing

The CuPCMT protein was digested with three proteolytic agents, viz., Trypsin, Chymotrypsin and CnBr [31]. The digests were desalted with ZipTip C_{18} matrix tips and were submitted to MALDI TOF MS/MS analysis. Analysis by the in-line GPS explorer software gave a list of possible matches along with score and peptide sequence. These peptide sequences were aligned with each other as well as with PCMT homologs manually to work out the sequence.

2.3.12. Nucleotide sequencing

The protein sequence deduced by de novo sequencing techniques was back-translated by EMBOSS Backtranseq tool at the EBI website against the codon usage data of the closest related species *Candida albicans* [32]. The nucleotide sequence obtained was used to design forward and reverse primers. Total RNA from early stationary phase cells of *C. utilis* was obtained using the RNeasy Mini Kit from Qiagen following the manufacturer's protocol. The CuPCMT mRNA was isolated from total RNA employing the SuperScript® One-Step RT-PCR System with Platinum® Taq DNA Polymerase from Invitrogen™, Life Technologies, USA. The PCR cycle is as follows – cDNA synthesis (1 cycle): 55 °C for 20 min, denaturation (1 cycle): 94 °C for 2 min, PCR amplification (40 cycles): 94 °C for 15 s (denature), 55–65 °C for 30 s (anneal), 68 °C for 1 min (extend) and a final extension of 5 min at 68 °C. The PCR product was sent to Xcelris Genomics, Hyderabad, India for sequencing.

2.3.13. In silico analyses of the protein and nucleotide sequences

The nucleotide sequence was subjected to BLAST with NCBI blastn suite against the non-redundant (nr) database [33]. The sequence was aligned with the published *C. utilis* genome database (*Cyberlindnera jadinii* genome portal) to determine the location of the gene within the genome [34,35].

The amino acid sequence was deduced from the EMBOSS Transeq tool at EBI. The amino acid sequence was subjected to BLAST with NCBI blastp suite as well as the cross genome database blastp at the *Candida* Genome Database [33,36]. Secondary structure prediction was done using the PSIPRED [37]. Conserved domains within the sequence were determined using the CD-search tool at NCBI [38].

Phylogenetic comparison between the PCMT sequence and eleven other PCMT sequences from representative organisms was performed by Clustal Omega tool using the default parameters [39]. The PCMT sequences chosen for analysis include Human (P22061), Bovine (P15246) and Rat (P22062) among mammals, *Drosophila* (Q27869) among insects, *Caenorhabditis* (Q27873) in nematodes, Wheat (Q43209) and *Arabidopsis* (Q42539) among Plants, *Neurospora* (Q7RWK6) and *Schizosaccharomyces* (Q9URZ1) among Fungi, *Helicobacter* (P56133) and *Thermotoga* (Q56308) among the bacteria. A phylogenetic tree was generated from the alignment result using the EvolView Tool [40].

2.3.14. Repair of in vitro aged proteins by CuPCMT

Four common cellular proteins were selected as candidate for demonstrating the repair ability – Immunoglobulin G from rabbit

serum (Sigma Aldrich I5006), Hexokinase from *Saccharomyces cerevisiae* (Sigma Aldrich H6380), Glutamate dehydrogenase from bovine liver (Sigma Aldrich G7882) and Cytochrome c from Equine heart (Sigma Aldrich C2506). The candidate proteins (0.5 mg) were subjected to *in vitro* aging for 10 days at 37 °C in an *in vitro* aging buffer as mentioned in Section 2.3.3. 0.25 mg aged proteins were incubated with PCMT and AdoMet for 2 h at 30 °C to induce protein repair. The enzyme activities of unaged, aged and repaired Hx and GDH were measured following protocols mentioned earlier. For Immunoglobulin G (IgG) and Cytochrome c (Cyt c), the repair was assessed by CD Analysis as mentioned earlier. The isoaspartate content of all sets were measured with the ISOQUANT isoaspartate detection kit.

2.3.15. *In vivo control of CuPCMT activity*

C. utilis cells were grown in 50 ml YPD media till early stationary phase (28 h, OD_{660} ~23). Cells were harvested by centrifugation at 500*g* for 5 mins. Supernatant was discarded and the pellets were washed twice with PBS. Washed pellets were redissolved in fresh YPD with the addition of 0–2 mM AdOx or 0–2 mM LiCl. Cells were grown for 24 h at 30 °C with mechanical shaking at 200 rpm. After 24 h, cells were harvested, lysed with glass beads and assayed for PCMT activity.

2.3.16. *Effect of in vivo manipulations of CuPCMT activity in C. utilis*

Intracellular ROS levels were measured with a cell permeable fluroscent probe 2′,7′-dichlorodihydrofluorescein diacetate (H_2DCFDA). Early stationary phase cells were subjected to treatment with 0, 0.5, 1, 1.2, 1.5, 1.8 and 2 mM AdOx or LiCl for 24 h as mentioned previously. To evaluate whether increased PCMT activity affect ROS generation levels, Δ*pcmt C. utilis* cells were incubated with similar concentrations of LiCl. Harvested cells (1×10^7 cells/ml) were resuspended in PBS with 100 μM H_2DCFDA. Samples were incubated for 45 min at 30 °C in dark, washed twice in ice-cold distilled deionized water and re-suspended in 1 ml PBS. Fluorescence intensity was measured by a BD LSRFortessa™ Cell Analyzer with excitation at 490 nm and emission at 518 nm.

2.3.17. *PCMT gene expression level in AdOx and LiCl incubated C. utilis cells*

Early stationary phase cells were subjected to treatment with 0, 0.5, 1, 1.2, 1.5, 1.8 and 2 mM AdOx or LiCl for 24 h as mentioned previously. After 24 h, cells were harvested from 4 ml cultures and total RNA was extracted using the RNeasy Minikit from Qiagen as mentioned previously. 1 μg RNA from each set was used to quantify PCMT expression under treatment with AdOx or LiCl. Primers forward 5′- TCAAATGCTGCTTTGTTTGG- 3′ and reverse 5′-TTTGAGCCAATTGTGATGGA-3′ were used to amplify a ~600 bp pcr product. β-actin was amplified to serve as a control with the forward primer 5′-GCCATTGCCACCATCAAGAC-3′ and the reverse primer 5′-CACACCAACCTCCTCATAAT-CCTTC-3′, yielding a 323 bp product. SuperScript® One-Step RT-PCR System with Platinum® Taq DNA Polymerase from Invitrogen™, USA, was used following the manufacturers protocol. The reverse transcription was done at 55 °C for 20 min followed by a denaturation step at 94 °C for 2 min. Amplification was carried out for 30 cycles at 94 °C for 45 s, 60 °C for 45 s and 68 °C for 90 s. Those steps were followed by a final extension of 5 min at 68 °C. RT-PCR products were analyzed on an 1% agarose gel stained with ethidium bromide.

2.3.18. *C. utilis cell survival assay under stress*

Stationary phase *C. utilis* cells (treated either with 0.8 mM AdOx or 1 mM LiCl separately) were subjected to four types of insults-oxidative stress for 200 min with addition of 30 mM H_2O_2, pH stress for 6 h with 0.1 mM Hydrochloric acid (pH 2.0), hyperosmotic stress for 40 min with 1.5 M NaCl and heat stress by incubating the cells at 42 °C for min. For each treatment an untreated set was prepared without addition of AdOx or LiCl which were also subjected to same stress conditions. A control set was prepared where stationary phase cells were subjected to incubation without treatment or stressor compounds. All four sets were incubated at 30 °C except the sets subjected to heat stress, with mechanical shaking of 200 rpm. Cell viability was evaluated by MTT colorimetric assay. Cells were grown in standard YPD medium to early exponential or stationary phase and washed with water. Cell density was adjusted to 2×10^7 cells/ml. Cells from 1 ml suspension were harvested and resuspended in 0–4 ml 10% MTT (3-(4,5-dimethylthiazoyl-2-yl) 2,5-diphenyltetrazolium bromide). The mixture was incubated at room temperature with shaking for 2 h under dark. After 2 h cells were harvested and resuspended in 1 ml acid 2-propanol (0–0.4 M HCl in 2-propanol). The suspension was agitated for 10 min and centrifuged at 8000 r.p.m. The OD_{540} of the supernatant was then measured.

Cell survival under each stress was evaluated by flow cytometry using an Annexin V-FITC Apoptosis Detection Kit from Sigma, USA. Cells from each set were harvested and washed as mentioned earlier. Cells were resuspended in PBS allowing a concentration of approximately 10^6 cells/ml. Annexin V-FITC and Propidium Iodide (PI) were added following manufacturers protocol. Cells were incubated for 30 mins before analysis in a BD LSRFortessa™ Cell Analyzer with excitation at 488 nm and emission at 530 nm.

At the end of each stress treatment, 18 mg wet weight of cells from the control and treated sets were harvested. Cells were lysed with glass beads and lysates were investigated for their isoAsp contents using the ISOQUANT® Isoaspartate detection kit following the radioactive method (Promega, USA). An enzyme blank reaction was set up to nullify the PCMT activity in experimental sets.

2.3.19. *2-dimensional gel electrophoresis*

Stationary phase *C. utilis* cells were treated with 1 mM AdOx for 24 h before they were harvested. Yeast cells, both treated and untreated, were lyophilized prior to protein extraction. Protein extraction was done following a published protocol by Kolkaman et al. [41]. In short, 80 mg dry weights of yeast cell were vortexed with acid washed glass beads in 6 × 60 s pulses with 30 s intervals on ice. Lysed cells were resuspended in 650 μl of hot (95 °C) SDS sample buffer (0.1 M Tris–HCl, pH 7.0, 1.0% (w/v) SDS, 10 μl protease inhibitor cocktail). The sample was boiled for 10 min and subsequently cooled on ice. 75 μl of a DNase and RNase solution (1% (w/v) DNase I, 0.25% (w/v) RNase A, 50 mM MgCl2, 0.5 M Tris-HCl, pH 7.0) was added and incubated on ice. The sample was diluted by adding 2.0 ml of a solubilization buffer (2 M thiourea, 7 M urea, 4% (w/v) CHAPS, 2.5% (w/v) DTT, 2% (v/v) carrier ampholytes, pH 3–10 nonlinear, and 10 μl protease inhibitor cocktail). The samples were shaken for 18 h on a roller mixer at room temperature followed by clearing through centrifugation at 3000*g*. Protein concentration was determined with a Bradford protein assay using BSA as a standard. The cleared supernatants were stored in aliquots at −80 °C.

100 μg of protein (125 μl) was loaded on a 7 cm Immobiline Dry-Strip pH 4–7 (Amersham Biosciences, USA). Strips were rehydrated for 13–15 h at room temperature, followed by IEF in a a PROTEAN IEF Cell (BioRad), with the current limited to 100 μA per strip, at 20 °C, for a total of 14,000 volthours. Prior to the second dimension, the IPG strips were incubated for 20 min in equilibration buffer 1 (50 mM Tris HCl, 6 M urea, 30% glycerol, 2% SDS, 10 mg/ml DTT), followed by 20 min incubation in equilibration buffer 2 (50 mM Tris HCl, 6 M urea, 30% glycerol, 2% SDS, 25 mg/ml IAA).

Second-dimension electrophoresis was performed on laboratory-cast 4–12% SDS-polyacrylamide gels in a BioRad Mini Protean 3 system. The IPG strips were placed on top of the polyacrylamide

gels and sealed with a solution of 1% (w/v) agarose containing a trace of bromphenol blue. Gels were run at 10 mA per gel for 15 min followed by 20 mA per gel until the bromphenol blue had migrated to the bottom of the gel.

2.3.20. On-blot methylation assay and identification of possible protein targets of CuPCMT

After electrophoresis, proteins were transferred onto PVDF membranes by Semi-Dry transfer in 25 mM Tris, 193 mM glycine, pH 8.3, 20% (v/v) methanol at 25 V, 4 °C for 30 min. After blotting, the membrane was immediately dried using 100% methanol in preparation for on-blot (^{3}H)-methylation. On-blot methylation for detection of isoAsp-containing proteins was carried out by following a published protocol by Morrison et al. [42], with certain modifications. Dried PVDF membranes holding transferred proteins were pre-wetted in 100% methanol for 45 s and rinsed in water before blocking in 10 mM Na-MES (pH 6.2), 2 mg/ml BSA for 30 min at room temperature. After blocking, the membrane was dried in 100% methanol, placed on a glass plate and immediately covered with 6 ml of methylation reaction solution1 warmed to 30 °C. The methylation reaction was allowed to proceed for 30 min before washing the PVDF membrane twice in 10 mM Na-MES, pH 6.2, 300 mM NaCl, and 0.05% Tween-20 for 10 min. Finally the PVDF membrane was washed in water for 5 min and then 100% methanol for 30 s prior to air-drying. Dried membranes were exposed to pre-flashed Kodak BioMAX XAR film for 2 weeks at −80 °C.

Gel corresponding to the Autoradiograph was lightly stained (20 min) with Coomassie Blue. Spots of interest from the two dimensional gel were excised. Gel pieces were destained in 50% acetonitrile, reduced with 20 mM dithiothreitol at 45 °C for 30 min, and alkylated with 100 mM iodoacetamide in 50 mM ammonium bicarbonate for 30 min at 37 °C in the dark. The processed gel spots were digested with trypsin at 37 °C overnight. The tryptic peptides were extracted twice with 50 μl of extraction solution (50% (v/v) acetonitrile and 0.1% trifluoro-acetic acid in water). The combined extracts were concentrated and desalted with ZipTip (C18, Millipore Inc., Bedford, MA) according to the product instructions. Tryptic digests were analyzed by MALDI-TOF mass spectrometry. Mass data were acquired by GPS explorer software and matched with MASCOT and Swissprot protein database to identify the proteins.

3. Results

3.1. A methyltransferase enzyme is responsible for the repair of isoaspartate moieties

Stationary phase *C. utilis* cells were incubated in media either containing 1 mM AdOx or 30 μM MG132 or 5 mM 3-methyladenine, for 24 h. Upon lysis the highest increase in intracellular isoaspartate content was observed in sets treated with 1 mM AdOx (357.62 pmoles isoAsp/mg protein)in comparison with the control set (134.56 pmoles isoAsp/mg protein) (Fig. 2A). Sets treated with MG132 and 3-methyladenine exhibited much less increase in isoAsp content in comparison with sets treated with AdOx.

Untreated Δ*pcmt C. utilis* cells were lysed with a general lysis buffer (LB) and the lysate was subjected to *in vitro* aging in four sets with the addition of four different protease inhibitors in each set, which were then incubated at 37 °C for 72 h. In all four sets with protease inhibitors, IsoAsp content was seen to be increasing. Most increase was noted when treated with EDTA, from 298.6 pmoles/mg protein to 488.62 pmoles/mg protein (Fig. 2B).In sets incubated with other proteases. Increase in isoAsp levels was noted but they were less compared to the set with EDTA (Fig. 2B).

Cells from each growth phase of *Candida utilis* were harvested, lysed and checked for the PCMT activity in order to identify the window where PCMT activity would be highest. Plotting the PCMT activity along the growth curve of yeast *C. utilis* revealed that PCMT activity was highest at O.D. (660 nm) ~23 which was achieved in around 28 h. After 28 h, PCMT activity remained steady in the stationary phase (Fig. 3). Purification steps were initiated from cultures that have reached O.D. (660 nm) ~23–25.

Highest relative activity of PCMT was recorded in 30–50% ammonium sulfate fractionation. Almost 6.46-fold increase in purification with 88.9% yield of the total activity was achieved at this step (Table 1). This step of purification saw a PCMT specific activity of 2444.67 U/mg. During the first HPSELC in BioSuite 125 Column, PCMT activity eluted out between 18 and 24 min with maximum activity eluting out at 21 min (data not shown). The specific activity of PCMT was detected to be around 7322.15 U/mg with almost 18.42-fold increases in purification and 82.5% yield of the total activity (Table 1). The pooled and concentrated fractions from the previous step were injected into the Protein-Pak 125 column. PCMT activity eluted out between 12 and 16.5 min and

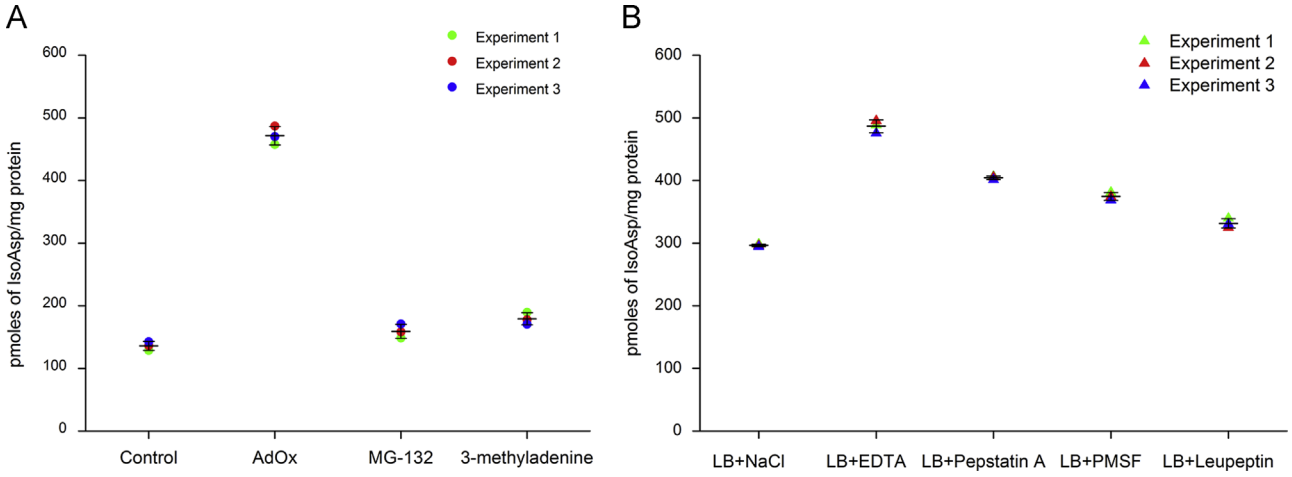

Fig. 2. Nature of Isoaspartyl repair in *C. utilis*. (A) *C. utilis* cells were grown till early stationary phase. Cells were harvested and re-dissolved in fresh YPD media containing 1 mM oxidised adenosine periodate (AdOx), 30 μM MG-132 or 5 mM 3-methyladenine. Cells were incubated for 24 h. Cytosolic extracts were prepared and Isoaspartyl levels were detected as mentioned in methods Sections 2.3.1 and 2.3.2 respectively. *Y*-axis denotes pmoles of isoAsp per mg extract. (B) Cytosolic extracts of early stationary phase Δ*pcmt C. utilispcmt* cells were prepared and incubated at 37 °C for 72 h with various protease inhibitors. After incubation isoAsp content were detected for each set. *X* axis denotes the combination of protease inhibitors used along with Lysis Buffer (LB). *Y* axis denotes the isoAsp levels as pmoles of isoAsp per mg cytosolic extract. Data presented is from three independent experimentation sets. The horizontal bars indicate the average (Mean), and the error bars represent standard deviation (S.D.).

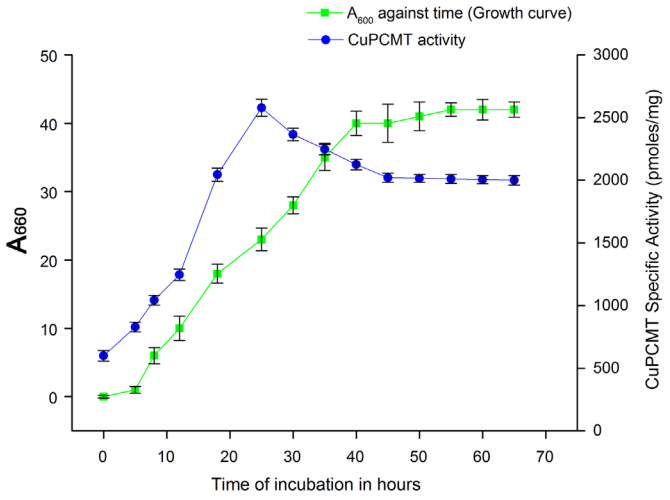

Fig. 3. Distribution of PCMT activity along the growth curve of *C. utilis*. *X*-axis denotes the time of incubation. Primary *Y*-axis denotes optical density of the culture at 660 nm. The resulting line graph is the growth curve of *C. utilis*. Secondary *Y*-axis denotes PCMT specific activity. Data represented is the mean of three independent experimentation sets and the error bars represent standard deviation (S.D.).

the protein peak had a retention time of 13.6 min (data not shown). The final purification fold and maximum yield of the enzyme in this step are 43.41 and 76.06 respectively. The specific activity of this final stage is 17008.97 U/mg (Table 1).

Purification was validated by HPRPLC, HPSELC, SDS PAGE and MALDI TOF (Fig. 4). HPRPLC and HPSELC show single peaks when purified protein was injected (Fig. 4A and B). The approximate molecular weight of the purified PCMT enzyme was determined from HPSELC column and SDS PAGE to be ~25 kDa, from the standard calibration curve of the Protein-Pak column (Fig. 4B) and the relative migration (R_f) values of the molecular weight standards (Fig. 4C) respectively. The exact molecular weight of the purified native CuPCMT came to 25.4 kDa from MALDI TOF MS analysis of the whole protein (Fig. 4D).

3.2. Basic biophysiscal, biochemical, sequence and structural attributes of the purified CuPCMT were worked out

The optimum temperature for CuPCMT enzyme activity was 30 °C and the enzyme was most stable between the temperatures 30–40 °C (Fig. 5A). The enzyme exhibited optimum activity at pH 7.0 and was most stable between pH values 6.5 and 7.5 (Fig. 5B).

Substrate specificity assays demonstrated that CuPCMT displayed activity against proteins and peptides containing isoAsp residues (Table 2). PCMT activity was lowest against BSA but it doubled when the BSA was aged upon incubation in *in vitro* aging buffer. Highest activity was found to be against the IsoAsp DSIP (Table 2).

The enzyme kinetics parameters like K_m, V_{max} and K_{cat} were determined for PCMT (Table 3). K_m for the methyl group donor AdoMet was 3.5 μM and for methyl group acceptor isoAsp DSIP it was 30.42 μM. V_{max} for the same substrates were 50250.86 pmols/min/mg and 50352.99 pmols/min/mg respectively. Catalytic turnover or K_{cat} for AdoMet was found to be 203.85 s^{-1} and 233.3 s^{-1} for Iso-Asp DSIP. The inhibitory constant or K_i against AdoHcy was 0.5 mM (Table 3).

The deduced nucleotide sequence was submitted to NCBI Nucleotide database with accession number KMO23327. Blastn run against NCBI non-redundant Nucleotide database revealed maximum similarity with *Schizosaccharomyces pombe* 972 h protein-L-isoaspartate O-methyltransferase Pcm2 (predicted) (pcm2), mRNA (NM_001020442.2) with an E-value of 3e-11 (data not shown). The nucleotide sequence was aligned against the published *Cyberlindnera jadinii* assembly scaffolds database to assign a gene locus. The deduced nucleotide sequence showed similarity with scaffold 1 between 80 and 152 bp (data not shown).

The amino acid sequence of the PCMT was determined following de novo sequencing by MALDI TOF MS/MS analysis. The sequence was consisting of 232 amino acids. The protein sequence along with the Adomet binding domain predicted from CD Search tool at NCBI is depicted in Fig. 6A, AdoMet binding domains being underlined in red.

Secondary structure of the purified protein was worked out by deconvoluting the CD spectra (Fig. 6B). The protein was predominantly an alpha helical protein as depicted in Table 4. The sequence was run with the PSIPRED software and the secondary structure was predicted by designating regions most likely to form alpha helices, beta strands and random coils (data not shown). Predicted percentages of α-helix, β-sheet and random coil are compared with experimentally determined percentages in Table 4.

The Conserved Domain Database search at NCBI displayed that the protein belongs to the AdoMet dependent MTase Superfamily and a PCMT like conserved domain was detected within the sequence (Fig. 6C). Protein BLAST searches were performed against the non-redundant protein database at NCBI and against the *Candida* Genome database. The top hits in NCBI were against protein L-isoaspartyl methyltransferases from various sources. Most similarity was seen with PCMT from *Schizosaccharomyces pombe* with an E-value of 2e-73 (data not shown). BLAST search against the *Candida* Genome Database returned matches with sequence hits that are either methyltransferases as well as predicted methyltransferases containing PCMT domain from various *Candida* species (data not shown).

Eleven homologous sequences of PCMT from various source organisms were chosen for phylogenetic comparison with the amino acid sequence of the purified PCMT from *C. utilis*. Multiple alignment data from the Clustal Omega Tool was used to construct a Phylogenetic Tree (Fig. 6D). The resulting tree was a Rooted Cladogram constructed using a Distance Matrix based method. The numbers beside each branch represents the distance values for each. The distance values represent the number of substitutions as a proportion of the length of the alignment.

Table 1
Purification of PIMT from *C. utilis*. Data represented are the average of three sets of experimentations.

Steps	Total volume (ml)	Total protein (mg)	Total activity (pmols/min/ml)	Specific activity (pmols/min/mg)	Fold	Yield (%)
1. Lysate	27.6 ± 2.5	270 ± 2	106879.17 ± 3368.39	401.43 ± 18.3	1	100
2. Ammonium Sulphate (30–50%)	10 ± 2	38.16 ± 1.04	94296.07 ± 949.6	2444.67 ± 331	6.46 ± 0.45	88.9 ± 0.78
3. HPLC – Biosuite 125	14.6 ± 3.6	15 ± 3	88994.28 ± 284.6	7322. 15 ± 445.42	18.42 ± 0.69	82.4 ± 1.20
4. HPLC – ProteinPak 125	17.4 ± 2	7.6 ± 2.5	74736.19 ± 98.69	17008.97 ± 681.36	43.41 ± 1.37	76.06 ± 1.5

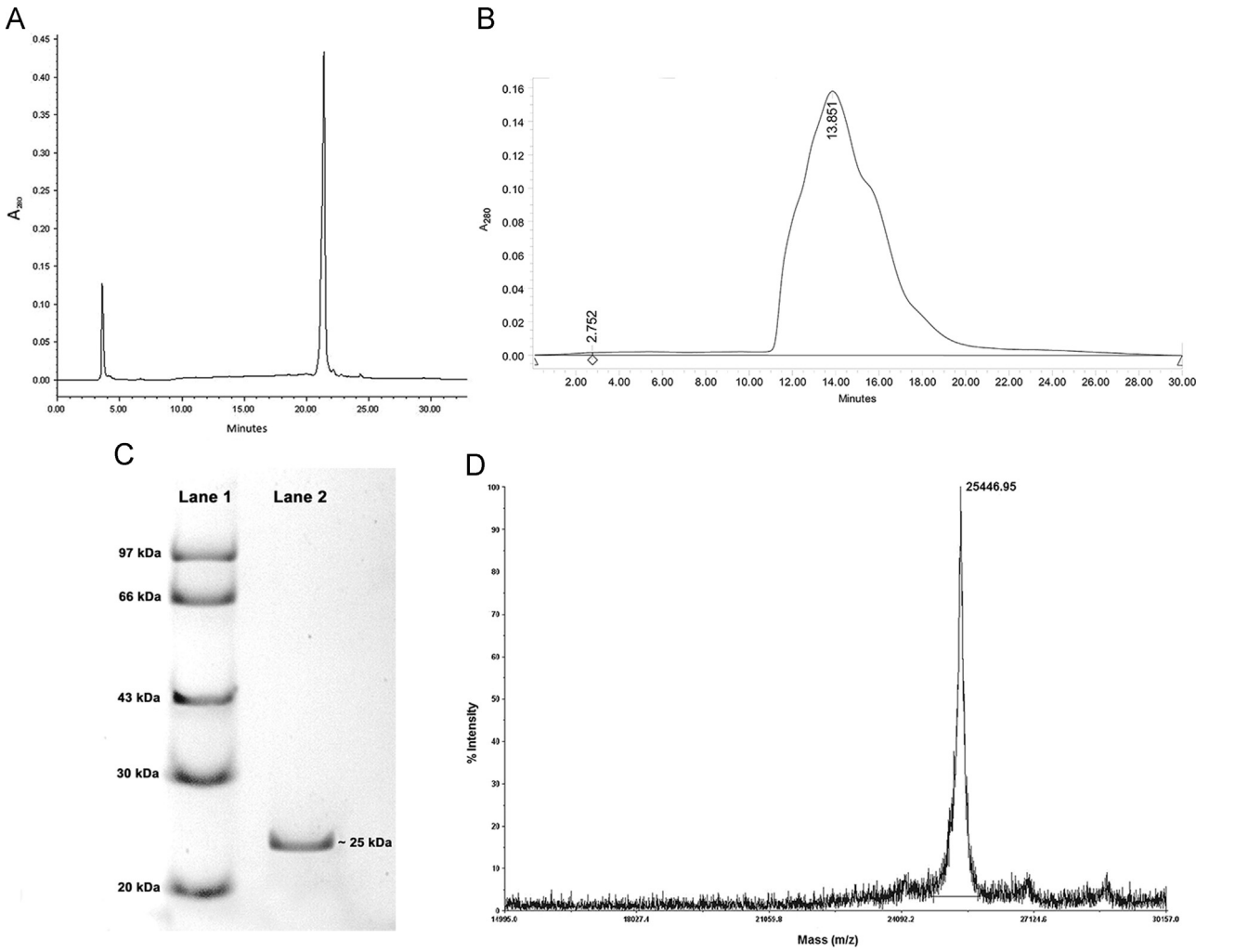

Fig. 4. Purification validation and molecular weight determination of purified CuPCMT**.** A. HPRPLC of purified PCMT in DeltaPak C4 column, Waters. The chromatogram denotes a single peak eluting at 21.5 min. *X*-axis denotes elution time in minutes and *Y*-axis denotes absorbance at 280 nm. The first peak is an artifact and was also observed in blank runs. B. HPSELC of the purified PCMT in Protein Pak 125 shows a single peak with retention time of 13.81 min corresponding to ~25 kDa according to the calibration curve of the column. C. SDS PAGE analysis was performed with 30 μg of purified CuPCMT protein as described in Section 2.3.8. Lane 1 shows low molecular weight standards from GE healthcare (Catalog no. 17-0446-01). The respective molecular weights f the standards are designated on the left of each band. 30 μg CuPCMT was loaded on to lane 2 which shows a single band with molecular weight of 25 kDa; D. MALDI TOF MS analysis of the whole purified protein exhibited a single spectrum indicating the true molecular weight of PCMT as 25.4 kDa.

3.3. *In vitro structural and functional repair of cellular proteins were achieved with CuPCMT*

The four candidate proteins were subjected to *in vitro* aging followed by repair of the aged proteins upon incubation with PCMT and AdoMet. Repair efficacy of the PCMT from *C. utilis* against enzymes Hx and GDH was demonstrated in terms of enzyme reactivation as well as isoAsp content (Fig. 7A and B). *In vitro* aging reduced Hx activity to 48% while after incubation with PCMT Hx activity increased to 76%. IsoAsp content was highest for the aged Hx protein at 0.58 pmoles/ pmole protein which was reduced to 0.36 pmoles/pmole proteins on repair (Fig. 7A). A similar scenario was observed with GDH. Aging reduced GDH activity to 50% and incubation with PCMT revived activity to 62%. IsoAsp content of control, aged and repaired GDH are 0.092, 0.43 and 0.19 pmoles/pmole protein (Fig. 7B). *In vitro* repair of IgG and Cytc were demonstrated by CD analysis in terms of molar ellipticity and isoAsp content. Fig. 7C represents the comparison between the CD spectra of native, deamidated and repaired IgG. Maximum structural variation occurred between wavelengths 215–220 nm. IsoAsp content was found to be increasing from 0.089 pmoles to 0.82 pmoles upon aging which decreased to 0.48 pmoles in repaired sets (Fig. 7D). From the comparative CD spectra of native, aged and repaired Cytc, it can be seen that aging induces an increase in molar ellipticity which decreases upon repair with PCMT (Fig. 7E). Change in molar ellipticity is reflected in the isoAsp content of the protein which increases to 0.39 pmoles and then decreases down to 0.092 pmoles/ pmole protein (Fig. 7F).

3.4. *PCMT expression correlates with cell survivability under stress*

Stationary phase *C. utilis* cells (A_{660}~23) were incubated for 24 h either with 0–2 mM AdOx or with 0–2 mM LiCl. As evident from Fig. 8A, maximum inhibition of PCMT activity was achieved by 0.8 mM Adox. It is also apparent that maximum enzyme activity was stimulated by 1.2 mM LiCl (Fig. 8A). Further experiments were conducted by incubating the cells in either 0.8 mM AdOx or 1.2 mM LiCl (Fig. 8A). ROS generation was measured in cells incubated in both AdOx and LiCl. In both the cases, ROS levels were seen to increase. In case of AdOx incubated cells the rise of ROS concentration in cells was seen to be gradual, and a maximum of 70% cells (Fig. 8B). At the concentration 0.8 mM, only 24.15% were showing H_2DCFDA fluorescence. In cells incubated with LiCl, ROS generation was much more severe. At maximum LiCl concentration almost 100% of cells were showing H_2DCFDA fluorescence

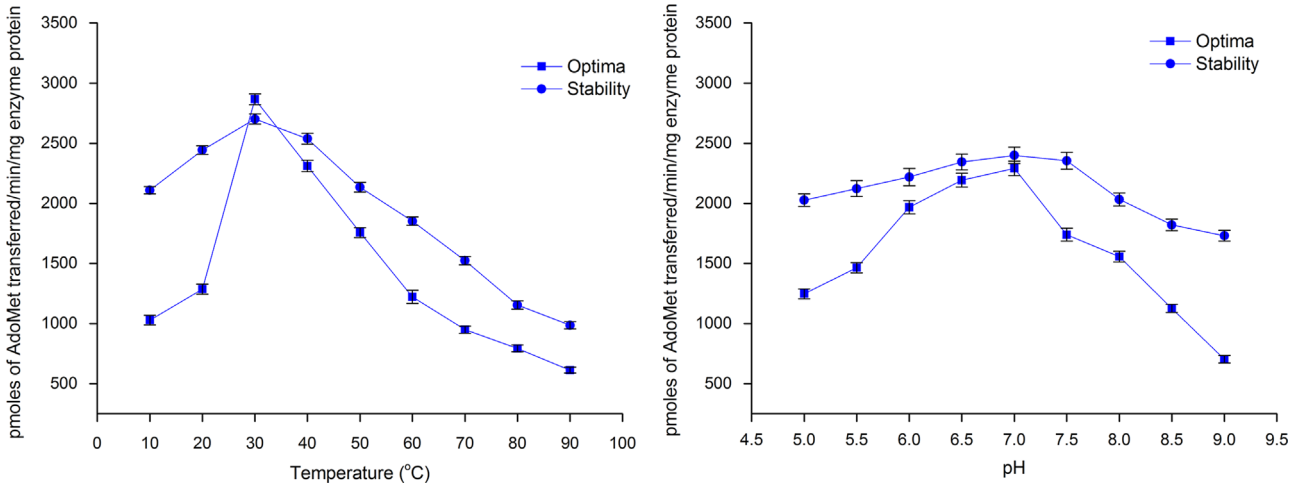

Fig. 5. Temperature and pH dependence of purified CuPCMT. (A) Temperature stability of the native CuPCMT was determined by pre-incubating the enzyme proteins in different temperatures (10–90 °C) for 30 min and then measuring the enzyme activity at 30 °C. To obtain the temperature optima of the CuPCMT enzyme, the enzyme activity assay was conducted in different temperatures (10–90 °C). *X*-axis denotes the incubation temperatures and *Y*-axis denotes the CuPCMT specific activity in pmoles of methyl groups transferred per minute per mg protein. (B) pH stability of the native CuPCMT was determined by pre-incubating the enzyme proteins in different pH buffers (5.0–9.0) for 30 min and then measuring the enzyme activity at pH 6.8. To obtain the pH optima of the CuPCMT enzyme, the enzyme activity assay was conducted in different pH buffers (5.0–9.0). *X*-axis denotes the incubation pH and *Y*-axis denotes the CuPCMT specific activity in pmoles of methyl groups transferred per minute per mg protein. Data represented in the figure is the mean of three independent sets of experimentations and the standard deviation is denoted by error bars.

Table 2
Activity of Purified Native Protein L-Isoaspartyl Methyltransferase from *C. utilis* toward Different L-Isoaspartate- containing Peptide and Protein Substrates. The endogenous activity in the absence of methyl-accepting substrate is subtracted. Enzyme concentrations used for the assays was 35 μM. All reactions were done in triplicates. Data represented in the table is the mean from three independent experimental states with ± range.

Substrate	Concentration of substrates (mM)	Specific activity (pmol/min/mg protein)
BSA	0.2	65.23 ± 1.23
	0.5	103.6 ± 2.6
	1	363.8 ± 1.02
Deam BSA*	0.2	125.48 ± 4.16
	0.5	504.5 ± 5
	1	1243.96 ± 6.9
Ovalbumin	0.2	542.5 ± 4.20
	0.5	1458.6 ± 35.8
	1	2993.7 ± 86.3
γ- Globulin	0.2	301.5 ± 9.6
	0.5	864.1 ± 12.6
	1	1741.5 ± 22.6
IsoAsp DSIP	0.2	9822.4 ± 102.6
	0.5	24,582.6 ± 333.96
	1	65,540.93 ± 1024.5

* Deamidated BSA or Deam BSA was generated by incubating BSA for 10 days at 37 °C in the *in vitro* aging buffer mentioned in the Materials and Methods section.

Table 3
Kinetic Rate Constants of Purified Native Protein L-Isoaspartyl Methyltransferase from *C. utilis*. Methyltransferase reactions were performed as described under Materials and Methods in triplicate using varying concentrations of the substrates Iso-Asp DSIP (0–0.1 mM) and [^{3}H]AdoMet (0–10 μM). For the reactions with variable peptide concentrations, AdoMet was used at a concentration of 40 μM whereas for variable AdoMet concentrations, Iso-Asp DSIP was used as a substrate at 0.3 mM. 10 μl enzyme protein was used for all experiments. The kinetic parameters of the enzyme were calculated by fitting the data to the Michaelis–Menten equation using the Origin (Version 8.5) software. K_i was determined by fitting the data into Lineweaver–Burke plots for the different concentrations of AdoHcy used. Values represent mean ± SD.

Kinetic parameters	AdoMet	IsoAsp DSIP
K_m	3.5 ± 0.05 μM	30.42 ± 0.07 μM
V_{max}	50, 250.86 ± 2,563.4 pmols/min/mg	50, 352.99 ± 3,428.6 pmols/min/mg
K_{cat}	203.85 s^{-1}	233.3 s^{-1}
K_i (AdoHcy)	0.5 ± 0.012 μM	–

(Fig. 8C). At 1.2 mM LiCl, 70% of the cells were generation ROS (Fig. 8C). In Δ*pcmt C. utilis* cells, ROS levels were found to be higher. At 1 mM LiCl concentration, 80% Δ*pcmt* cells were seen to show H_2DCFDA fluorescence compared to 53% in wild type cells (Fig. 8C). Semi-quantitative RT-PCR analysis of LiCl incubated cells show a gradual increase in transcript concentration upto 1.2 mM beyond which it gradually declined (Fig. 8D). AdOx treatment did not show any increase in transcript levels (data not shown). In control sets, AdOx treatment increased the isoAsp levels from 135.4 pmoles/mg protein to 277.1 pmoles/mg protein (Fig. 8E). Under stress conditions, AdOx treatment generally increased isoAsp content by at least 60%. Cells treated with 0.8 mM AdOx accumulated 370.08, 415.8, 405.8 and 345.4 pmoles/mg total cellular proteins under conditions of oxidative, pH, hyperosmotic and heat stress respectively. In sets treated with LiCl, cells accumulated less isoAsp than those without treatment, 79.89 vs. 130.44 pmoles/mg protein (Fig. 8E).Under LiCl treatment isoAsp levels were generally lowered by 45%, 46.6%, 44.4% and 40.6% in case of oxidative, pH, hyperosmotic and heat stress (Fig. 8F).

Cellular role of PCMT induction and inhibition was demonstrated by a cell viability assay as well as by FACS analysis. *C. utilis* cells when subjected to oxidative stress with H_2O_2 for 200 min, 85% of the AdOx treated population died whereas LiCl treatment promoted cell survival by 20% when compared to the untreated sets (Fig. 9A). FACS analysis revealed that LiCl treatment increased cell survival by 12% compared to the untreated set (Fig. 9B). Under pH stress with HCl, AdOx treatment failed to maintain cell viability whereas LiCl treatment helped maintain cell viability by 21% (Fig. 9C). In case of pH stress, cellular necrosis was seen to be the preferred cell death pathway. LiCl treatment reduced necrotic cell death by 16% in comparison with untreated cells under stress, whereas, AdOx treatment made cells susceptible to stress by 25% (Fig. 9D). In case of hyperosmotic stress with NaCl, at the end of 40 min, compared to the 32% cells in untreated set, 10% cell survived in the AdOx treated cells and 68% in LiCl treated sets (Fig. 9E).The same sets when analyzed with FITC-Annexin V staining followed by FACS analysis, demonstrated that in comparison with untreated sets, 55% of AdOx treated cells and 37.2% of

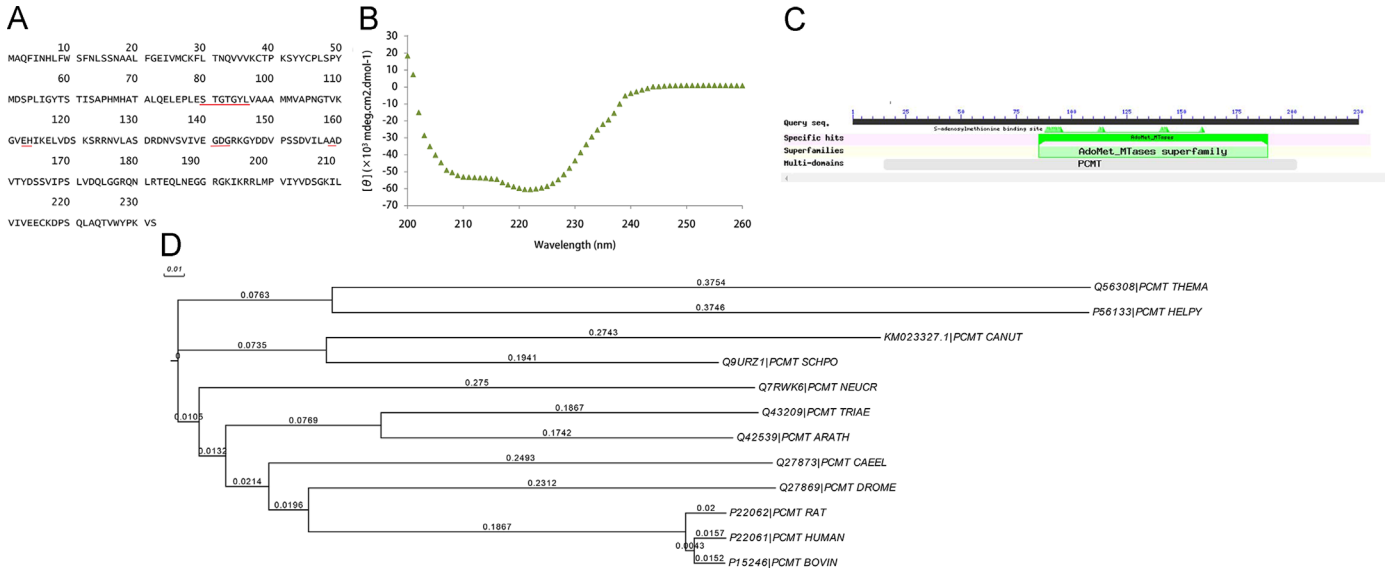

Fig. 6. Structural characteristics of the native CuPCMT. (A) Amino acid sequence of the CuPCMT was determined by MALDI TOF MS/MS analysis. The AdoMet binding sites within the sequence were determined by analyzing the sequence with online tool PSIPRED and are underlined in red; (B). Circular dichroism spectra of the purified PCMT. The *X*-axis represents the wavelength in nm and *Y*-axis represents molar ellipticity (θ). Deconvolution of the CD data by CDNN software gave percentages of the α-helix, β-sheet and random coil. The predicted and experimentally determined percentages are listed in Table 4; (C). To validate the amino acid sequence for structural characteristics, it was analyzed by CD search tool from NCBI. The output image denotes the conserved domains detected within the amino acid sequence; D. Phylogenetic comparisons between PCMT from *Candida* and eleven homologs from different representative organisms by Clustal Omega tool gave a Phylogenetic tree in the form of a rooted cladogram. The abbreviations used are: THEMA: *Thermotoga maritima*; HELPY: *Helicobacter pylori*; CANUT: *Candida utilis*; SCHPO: *Schizosaccharomyces pombe*; NEUCR: *Neurospora crassa*; TRIAE: *Triticum aestivum*; ARATH: *Arabidopsis thaliana*; CAEEL: *Caenorhabditis elegans*; DROME: *Drosophila melanogaster*; BOVIN: Bovine.

Table 4
Comparison of the percentages of the various secondary structures in the model predicted at PSIPRED and experimentally deduced upon deconvoluting the CD spectra by CDNN software.

Secondary structure	Predicted (%)	Experimental (%)
α helix	29.5	33.04
β sheet	16.09	19.5
Random coil	54.35	47.39

LiCl treated cells underwent apoptosis (Fig. 9F). Under heat stress at 42 °C, AdOx treatment decreased cell viability by 18% compared to untreated sets under stress whereas LiCl treatment helped maintain cell viability by 15% compared to the same (Fig. 9G). Cell death was predominantly by apoptosis and 58% of total cells incubated in 0.8 mM AdOx underwent apoptosis. LiCl treatment reduced apoptotic cell death by 22% in comparison with untreated cells under stress (Fig. 9H).

3.5. Cellular substrates of PCMT in C. utilis were identified

C. utilis cells were grown upto early stationary phase and incubated for 24 h in presence or absence of 1 mM AdOx at 30 °C. Cell lysates, both treated and untreated, were subjected to 2-dimensional gel electrophoresis separately. The separated proteins were transferred onto PVDF membranes and on-blot methylation reaction was performed. The blots were exposed to X-ray films and kept in −80 °C. Control extracts show very low abundance of methyl accepting proteins in comparison with AdOx+ extracts (Fig. 10A and B). Thirty four spots (indicated by arrows) from corresponding 2D gels were excised and trypsin digested (Fig. 10B). Tryptic peptides were subjected to MALDI TOF MS for protein identification. MS data was matched with the Uniprot protein database against the fungi specific proteins. Of the thirty four proteins processed, twenty nine gave good matches with other fungal proteins and are listed in Table 5. Table 5 also enlist the biological function of each protein.

4. Discussion

Candida and *Saccharomyces* species belong to the same order Saccharomycetales and are around one third as divergent from each other [43,44]. They share several similarities in genetic and physical attributes, yet have developed distinct characteristics unique to each other over the course of evolution. *Candida* species like *Candida albicans* and *Candida glabrata* have developed adaptive features that render them unique as commensal organisms to warm blooded animals [45]. *C. utilis* has acquired differences in the both glucose and trehalose metabolism pathways compared to *Saccharomyces cerevisiae* [46–48]. *S. cerevisiae* lacks a PCMT homolog and has developed a non-repair pathway for minimizing isoAsp in the proteome. In our investigations, we report that *C. utilis* possesses a PCMT homolog that is employed in minimizing isoAsp accumulation. This difference may be part of certain adaptations that *C. utilis* may have acquired over time for better survival since more often than not it is competing for the same energy source as *S. cerevisiae* [49].

Despite of methylation by PCMT being a highly energy efficient repair mechanism against isoAsp induced protein impairment; some organisms like *C. elegans* and mice have also developed a protein degradation pathway in addition [50–52]. A similar protein degradation pathway mediated by metalloproteases is employed by the yeast *S. cerevisiae* [18]. The major strategy employed by most living organisms to remove detrimental isoAsp moieties from cellular proteins is by engaging a highly specific AdoMet dependent carboxy-methyltransferase. This enzyme targets isoAsp residues and catalyses the transfer of a methyl group to their alpha carboxyl chain to form a metastable methyl ester. Formation of this methyl ester marks the first step of the several spontaneous rearrangements that leads to repair of the peptide backbone (Fig. 1).

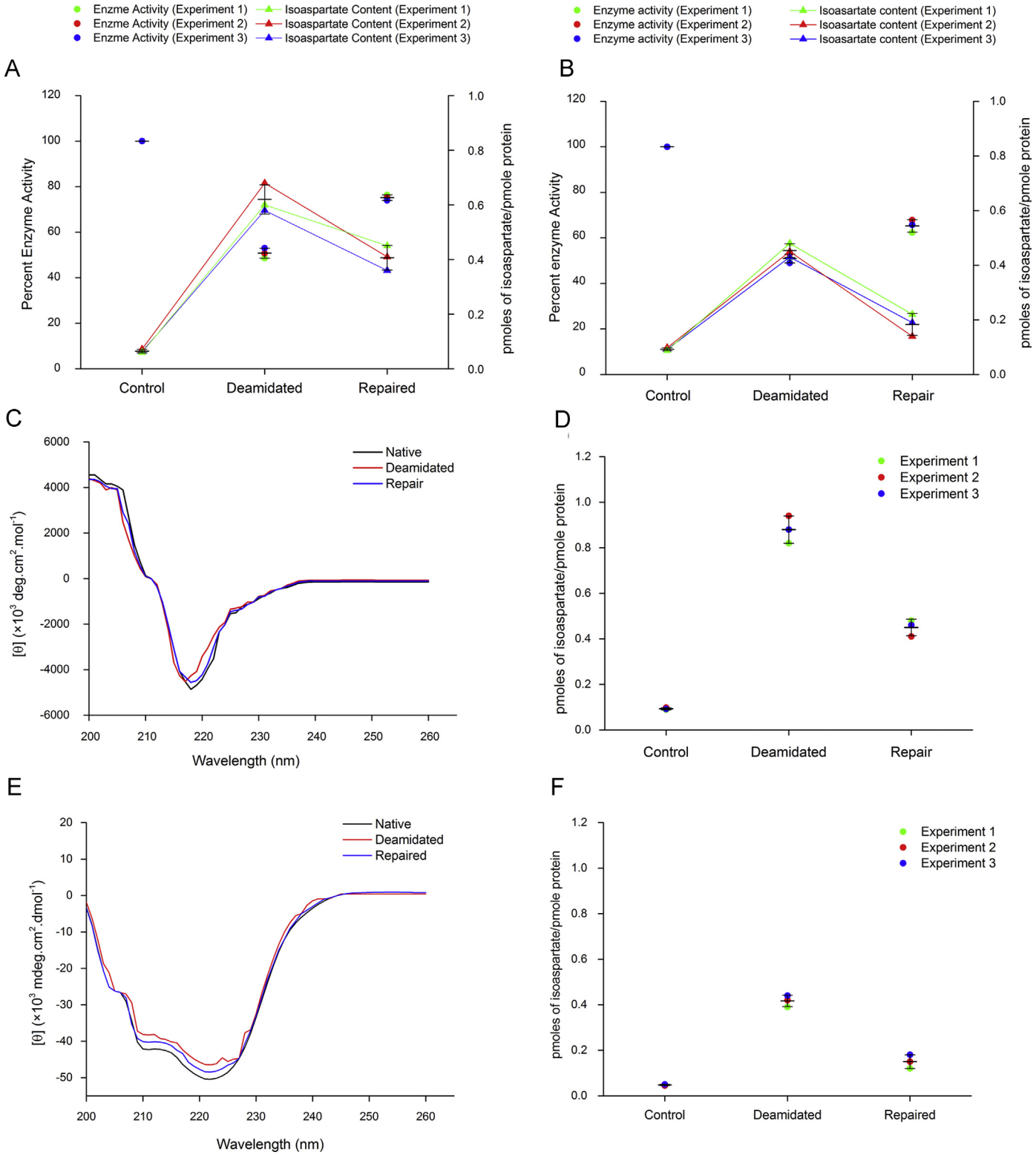

Fig. 7. *In vitro* repair efficiency of the native CuPCMT**.** Four candidate proteins were chosen based on their abundance in living organisms – two enzymes and two structural proteins. These proteins were aged *in vitro* and then subjected to a repair assay employing PCMT from *C. utilis* and AdoMet. IsoAsp levels of the control, aged and repaired proteins were also measured; (A) Enzyme reactivation assay for Hexokinase (Hx) demonstrates repair efficiency both in terms of enzyme activity as well as IsoAsp levels. The primary *Y*-axis denotes the enzyme activity in percentage where the activity of the native enzyme is designated as 100% and the secondary *Y*-axis represents isoAsp levels of the control, aged and repaired sets. (•) represent enzyme acivities and (−▲−) represents isoAsp contents. Data represented in the figure is the mean of three independent sets of experimentations and the standard deviation is denoted by error bars; (B) A similar representation for the enzyme reactivation assay of Glutamate dehydrogenase (GDH); (C) Repair of structural protein IgG was demonstrated in the form of CD spectra illustrating the changes in secondary structure upon aging and subsequent repair; (D) The isoAsp levels of control, aged and repaired IgG have been depicted along the *Y*-axis as pmoles of isoAsp/pmoles protein; (E) CD spectra comparison of the control, aged and repaired Cytochrome c (Cyt c) with *Y*-axis depicting the molar ellipticity (θ) and *X*-axis depicting the wavelength in nm; (F) The isoAsp levels of control, aged and repaired cytc have been depicted along the *Y*-axis as pmoles of isoAsp/pmoles protein. Data presented is from three independent experimentation sets. The horizontal bars indicate the average (Mean), and the error bars represent standard deviation (S.D.).

Table 5
Identification of possible substrates of PIMT in AdOx treated *C. utilis* cells. Coomassie-stained spots corresponding to major methyl acceptors (Fig. 10) were subjected to peptide mass fingerprinting by MALDI-TOF. The MS data was matched with the Uniprot protein database against all fungal proteins as well as with NCBI non-redundant protein database.

No.	Matched Protein	UniProt Accession number	Score	Function
1.	Ketol-acid reductoisomerase, mitochondrial	P38674	72	Amino acid biosynthesis
2.	Histidine biosynthesis trifunctional protein	O74712	74	Amino acid biosynthesis
3.	3-isopropylmalate dehydrogenase	P08791	90	Amino acid biosynthesis
4.	Pheromone-processing carboxypeptidase kex1	Q2UPI1	66	Apoptosis
5.	Adenylate kinase cytosolic	Q9HE76	72	ADP biosynthesis
6.	Fructose-1,6-bisphosphatase	Q9P8Q4	72	Carbohydrate metabolism
7.	Hexokinase I	O74996	70	Carbohydrate metabolism
8.	Glucan 1,3-beta-glucosidase	P29717	74	Cell-substrate adhesion
9.	Heat shock protein 90 homolog	P46598	77	Chaperon
10.	Enolase A	Q12560	72	Glycolysis
11.	Phosphoglycerate kinase	P00560	68	Glycolysis
12.	Phosphoglycerate mutase	P36623	70	Glycolysis
13.	Dolichyl-diphosphooligosaccharide–protein glycosyltransferase subunit wbp1	O59866	74	Glycosylation
14.	Guanine nucleotide-binding protein subunit beta-like protein	P83774	70	G-protein coupled receptor signaling pathway
15.	Phosphatidylinositol transfer protein PDR17	P53844	70	Lipid transport
16.	Polyadenylate-binding protein	Q5AI15	71	mRNA processing
17.	Protein involved in oxidative stress	A3GHN0	69	Oxidative stress response
18.	Copper chaperone for superoxide dismutase Sod1p	C4QWM2	70	Oxidative stress response
19.	Mitogen-activated protein kinase HOG1	Q92207	69	Oxidative stress response
20.	Protein farnesyltransferase subunit beta	P22007	68	Post translational modification
21.	Eukaryotic translation initiation factor 3 subunit 7-like protein	Q4Q6Y6	70	Protein synthesis
22.	Elongation factor 1-alpha	P02994	73	Protein sysnthesis
23.	Protein RER1	P25560	71	Protein transport
24.	GTP-binding protein YPT1	P01123	74	Protein transport
25.	Clan CA, family C1, cathepsin L-like cysteine peptidase	A2EMU7	68	Proteolysis
26.	Ribosome biogenesis protein RLP7 (Fragment)	P32101	84	Ribosome biogenesis
27.	Tubulin gamma chain	P53378	69	Structural protein
28.	60 S ribosomal protein L5	P26321	72	Structural protein
29.	AP-1-like transcription factor YAP1	P19880	68	Transcription regulation

Our experiments led us to believe that in *C. utilis*, both autophagic pathway and the proteasome pathways did not contribute to minimizing isoAsp levels since incubation with inhibitors MG-132 and 3-methyladenine did not lead to higher isoAsp accumulation (Fig. 2A). It could be seen from the same experiment that inhibiting the methyltransferase enzymes by a universal methyltransferase inhibitor AdOx led to increased isoAsp accumulation in *C. utilis* cells (Fig. 2A). Thus it could be concluded that in *C. utilis*, isoAsp levels are kept in check by a methyltansferase enzyme. Proteases were also seen to be contributing to lowering isoAsp accumulation in *C. utilis*. In absence of methyltransferase activity, *in vitro* aged cell lysates exhibited increased accumulation of isoAsp moieties. Sets incubated with EDTA showed slightly higher isoAsp accumulation than sets incubated with other protease inhibitors indication that metalloproteases contribute more towards degradation of isoAsp containing proteins than other proteases.

Accumulation of isoAsps has been generally correlated with progressive aging of the cells. *C. utilis* cells accumulate isoAsp residues in proteins as they progress through the cell cycle and maximum accumulation happens during stationary phase, after about 30 h of growth (data not shown). PCMT activity peaks at around 28 h and its levels are more or less maintained throughout the stationary phase indicating a possible role of PCMT in maintaining normalized cellular functions by minimizing isoAsp accumulation (Fig. 3).

PCMT was purified in its native form *C. utilis* by employing a simple approach. Two consecutive size exclusion HPLC steps coupled with a size based concentration step in between. Employment of just size exclusion chromatography reduced sample preparation time, increased reproducibility and decreased run time. Moreover, ion exchange chromatography is known to trigger protein aggregation due to the destabilization of the folding pattern of the native protein structure and may enrich certain protein modifications that inhibit native protein functions [53]. The success of the simple purification strategy was validated in RPHPLC, SEHPLC, SDS-PAGE and MALDI TOF analysis of whole native protein (Fig. 4). Comparison with earlier reports reveals that in terms of purification fold and protein yield, present method gave acceptable results. Purification fold was better than reported by Thapar and Clarke [54], for *Arabidopsis* which was 29 against 43.06 for *C. utilis* (Table 1). The purification fold was also comparable to the literature by David and Aswad [55], for PCMT from Rat which was 43 (Table 1). Protein Yield in the present method (78.50%) saw marked increase as compared to earlier reports from both *Arabidopsis* (3.2%) as well as Rat (20%) (Table 1) [54,55].

Optimum pH for CuPCMT activity was found to be 7.0 which seem in accordance with most published reports (Fig. 5A) [10,54,55]. While optimum ph for activity was consistent across different species, the optimum temperature for CuPCMt activity varied greatly among organisms. The CuPCMT was optimally active at 30 °C but reports from higher plants state the temperature optima to be around 45 °C [10]. PCMT from human exhibited a temperature optimum of 55 °C [10]. In bacteria like *Pyrococcus fruriosus* and *Thermotoga maritima*, PCMT activity required much higher temperature optima of 85 °C which is understandable given that they inhabit extremophilic environments [56,57]. This variation in temperature optima may be attributed to the different environmental adaptations for individual organisms. Temperature and pH stability of PCMT enzymes from various sources are indicative of the fact that the enzyme is suited to adapt to a wide range of physiological conditions. CuPCMT was seen to be most active between 30 °C and 50 °C beyond which enzyme activity saw a sharp decrease (Fig. 5A). Similarly limited temperature stability was observed in PCMT from other organisms like *Cicer*, *Caenorhabditis*, human and *E.coli* [10]. Stability of the CuPCMT enzyme at varied pH was much wider. In pH beyond 7.5 and 6.0 was

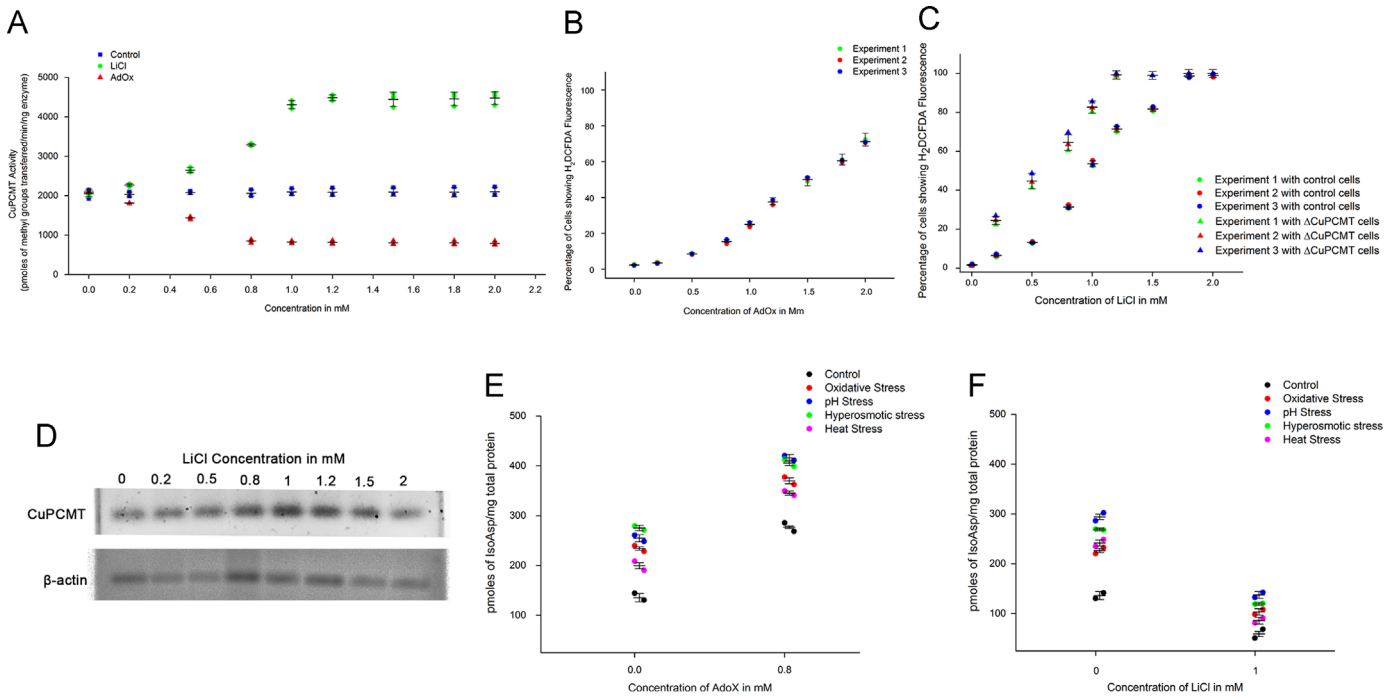

Fig. 8. *In vivo* regulation of CuPCMT in *C. utilis*. (A) *C. utilis* cells were grown up to early stationary phase and were incubated either with 0–2 mM AdOx or with 0–2 mM LiCl for 24 h. Post incubation cells were harvested, washed, lysed and checked for PCMT activity. *Y*-axis denotes PCMT activity in terms of pmoles of methyl groups transferred/min/ml enzyme. *X*-axis denotes both the concentration of AdOx and/or LiCl in mM. (B) ROS generation profile of cells treated by different concentrations of AdOx. The *X*-axis denotes the concentrations of AdOx used and the *Y*-axis denotes the percentage of cells showing H_2DCFDA fluorescence; (C) ROS generation profile of cells treated by different concentrations of LiCl. The *X*-axis denotes the concentrations of LiCl used and the *Y*-axis denotes the percentage of cells showing H_2DCFDA fluorescence; (D) Semi-quantitative RT-PCR analysis of CuPCMT transcript concentrations in cells incubated in different LiCl concentrations is exhibited in the top panel. β-actin transcript expression of the same sets of cells are designated in the lower panel; (E) Early stationary phase *Candida* cells were treated with 0.8 mM AdOx for 24 h followed by oxidative (●), pH (●), hyperosmotic (●) and heat (●) stress. Isoapartate levels of treated and untreated cells were worked out in terms of pmoles of isoAsp/pmole total cellular proteins. (F) Early stationary phase *Candida* cells were incubated in presence or absence of 1.2 mM LiCl for 24 h after which the cells were subjected to either oxidative (●), pH (●), hyperosmotic (●) and heat (●) stress. Intracellular isoAsp levels from control and treated sets were determined in terms of pmoles of isoAsp/pmole total cellular proteins. Data presented is from two independent experimentation sets. The horizontal bars indicate the average (Mean), and the error bars represent standard deviation (S.D.).

reduction in enzyme activity was not as drastic as changes in temperature (Fig. 5B). Similar reports were obtained from PCMT in higher plants and from extremophilic bacteria like *Thermotoga* and *Pyrococcus* [56,57]. The reason behind the difference between how temperature and pH affects enzyme activity may be that increasing temperature destabilizes the structural integrity of the protein more severely and may result in various unwanted modifications that hinder normal catalytic function. The changes in pH present as differences in ionic environments and may be more subtle to severely limit enzyme function.

The nucleotide sequence of the CuPCMT was obtained from a reverse approach by working out the protein sequence first. The whole genome of *Cyberlindnera jadinii*, the diploid, asexual, filamentous form of *Candida utilis*, has been sequenced [58]. Alignment of the nucleotide sequence with the available genome information of *Cyberlindnera jadinii* revealed a ~90 nucleotide long stretch of moderately similar sequence. The CuPCMT nucleotide sequence was also subjected to BLASTn search and it returned similarities with established or predicted PCMT sequences from various fungal, bacterial and plant sources predominantly. *In silico* analysis of the deduced amino acid sequence of the CuPCMT showed similar BLAST search results. A much more interesting result was obtained against the Candida Genome database where the BLAST search gave a list of sequence hits from various *Candida* species most of which were detected with either a methyltransferase domain or a PCMT domain or both. These proteins are yet to be annotated but the presence of the PCMT domain in most of them is a telltale sign that PCMT activity might be detected in these species of *Candida* as well. *In silico* analysis also corroborated the experimental data regarding secondary structure of the CuPCMT. Helix, sheets and coil percentages were found have comparable values (Fig. 6B, Table 4).

K_m for the CuPCMT against AdoMet was found to be higher compared to the human homolog (3.5 μM vs 2.2 μM) but lower compared to that from *Arabidopsis* (3.5 μM vs 9 μM) (Table 3) [54]. Affinity of the CuPCMT for AdoMet was comparable to the homologoues from prokaryotes like *Pyrococcus furiosus* (3.4 μM) or *Thermotoga maritima* (5.9 μM) [56,57]. A similar pattern was outlined when the 232 amino acid long CuPCMT protein sequence was compared with 11 other PCMT sequences from representative organisms from different groups for phylogenetic analysis. From Fig. 6D it is apparent that the CuPCMT from yeasts *C. utilis* and *Schizosaccharomyces pombe* has diverged from a node similar in length to that gave off the Prokaryotic PCMTs from *T. maritima* and *H. pylori*. The immediately neighboring branch gives off the PCMTs from a more evolved filamentous fungi *Neurospora crassa* followed by branching off of PCMT from higher plants. Highest divergence and farthest related to CuPCMT are the homologs from vertebrate animals. Combining the kinetic data and the phylogenetic comparison, it is evident that *C. utilis* being unicellular yeast, its cellular machinery as well as survival is similar to the bacterial counterparts like *T. maritima* or *H. pylori*. The changes in PCMT amino acid sequence that contributes towards divergence of the homologs from different organisms can be attributed to the complexity and abundance of downstream protein targets within individual organisms. The PCMT from *C. utilis* appears to represent the bridge between the prokaryotic PCMT and more evolved as well as specific eukaryotic counterparts.

To demonstrate the repair efficiency of the PCMT from *C. utilis*, four cellular proteins were chosen. Hexokinase and glutamate

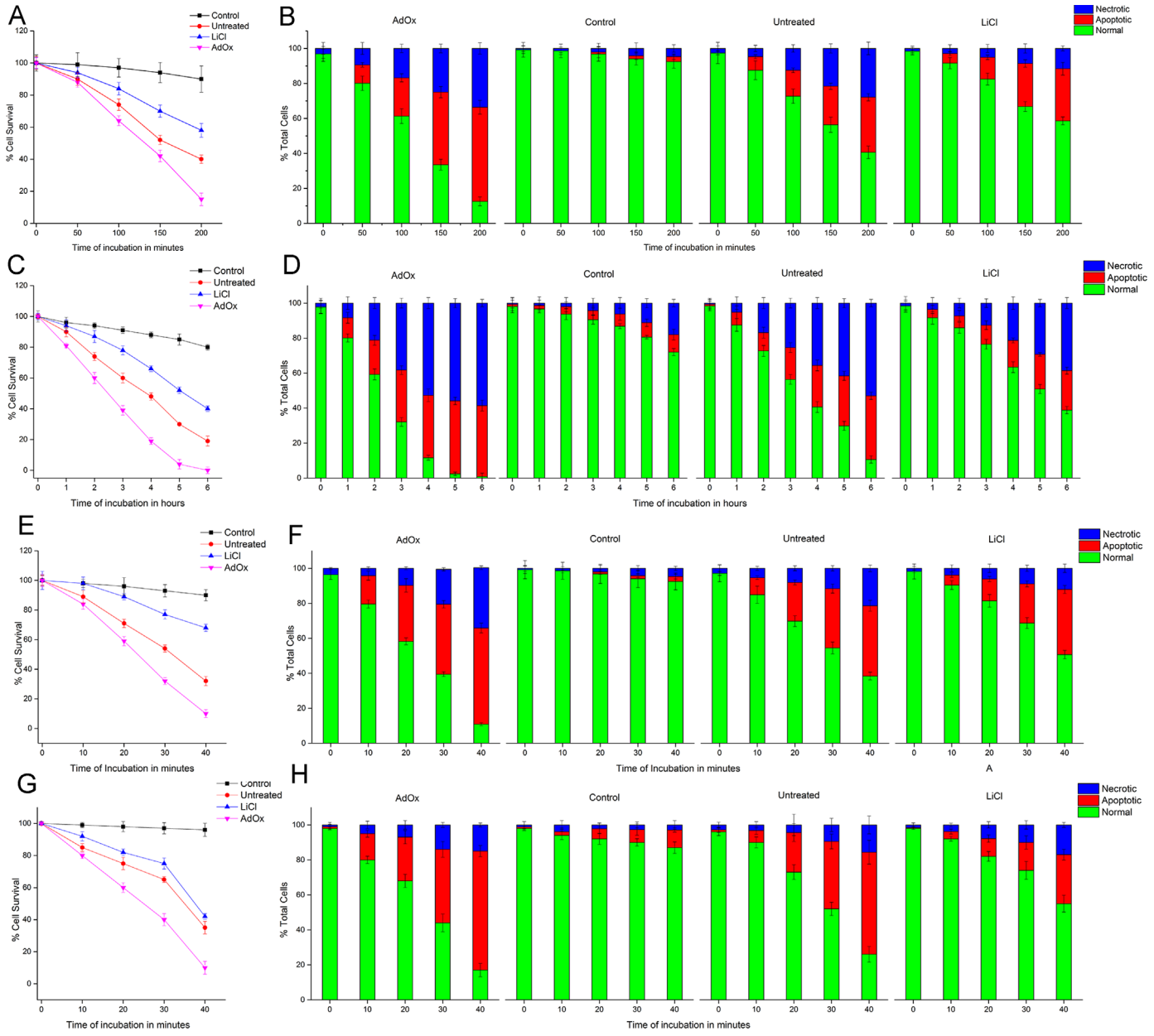

Fig. 9. Role of CuPCMT in cell survival under physiological stress**.** Control set represents early stationary phase *C. utilis* cells reconstituted in fresh YPD medium without AdOx or LiCl and not subjected to any stress condition. Untreated sets represent *C. utilis* cells reconstituted in media without AdOx or LiCl but subjected to the same stress condition as the treated sets. AdOx set represents *C. utilis* cells reconstituted in YPD medium containing 0.8 mM AdOx and subjected to stress condition. LiCl set represents *C. utilis* cells reconstituted in YPD medium containing 1 mM LiCl and subjected to stress conditions. *Candida* cells were subjected to oxidative stress by addition of 30 mM H_2O_2 for 200 min following 24 h incubation in either 0.8 mM AdOx or in 1 mM LiCl. Aliquots were drawn every 50 min. (A) Cell viability was assayed colorimetrically with MTT treatment and (B) cell death was monitored by flow cytometry analysis. *Candida utilis* cells were subjected to pH stress for with 0.1 mM Hydrochloric acid for 6 h following 24 h incubation in either 0.8 mM AdOx or 1 mM LiCl. Aliquots were drawn every 1 h. (C) Cell viability was assessed colorimetrically by MTT assay and (D) cell death by staining with Annexin V-FITC/PI followed by FACS analysis. *C. utilis* cells were subjected to hyperosmotic stress for 40 mins with 1.5 M NaCl following 24 h incubation in either 0.8 mM AdOx or in 1 mM LiCl. Aliquots were drawn at 10 min intervals from both treated and untreated sets and tested for (E) cell viability by MTT assay as well as (F) cell survival by flow cytometry after staining with Annexin V-FITC conjugate/PI. *Candida utilis* cells were subjected to heat stress at 42 °C for 40 min following 24 h incubation in either 0.8 mM AdOx or 1 mM LiCl. Aliquots were drawn every 10 min. (G) Cell viability was assessed colorimetrically by MTT assay and (H) cell death by staining with Annexin V-FITC/PI followed by FACS analysis.

dehyrogenase are metabolically important enzymes. Immunoglobulin G is a commercially important molecule which is prone to deamidation upon prolonged storage. Cytochrome c is a small molecule associated with the electron transport chain. Apart from these proteins or its homologs being abundant in living organisms, the sites and extent of isoaspartyl formation in these proteins have been reported in previously published reports [59–62]. Incubation with PCMT successfully reduced the isoaspartate levels in all four proteins. In case of the two enzymes, the aged forms regained their activity although complete reactivation could not be achieved (Fig. 7A and B). The disarrayed secondary structures showed partial refolding towards the original conformation after being incubated with PCMT and AdoMet (Fig. 7C and E). This *in vitro* repair assay established that CuPCMT is capable of reactivating the protein functions probably by initiating refolding of the abnormally linked proteins.

Young and co-workers [63] were able to downregulate PCMT expression in rat PC12 cells upon incubation in 10 μM AdOx for 24 h. AdOx is an *in vivo* methytransferase inhibitor that acts by increasing the AdoHcy levels that is a direct competitive inhibitor

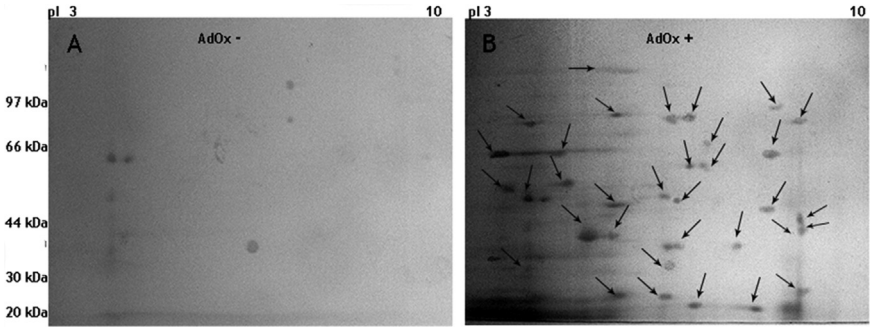

Fig. 10. Identification of intracellular protein substrates of CuPCMT. Stationary phase cells were incubated for 24 h with or without 1 mM AdOx following which the cells were lysed and the lysate (100 μg) were subjected to two dimesional gel electrophoresis. The proteins were blotted onto a PVDF membrane and the methyl accepting proteins were identified following an on-blot (^{3}H) methylation PCMT enzyme and AdoMet. Comparison between AdOx-and AdOx+extracts in A and B panels elucidate that inhibition of PCMT activity lead to increased accumulation of isoAsp moieties in cellular proteins. Methylated proteins are indicated by arrows. Corresponding spots in the gel were excised, trypsin digested and subjected to MALDI TOF MS/MS analysis. The possible downstream target proteins of PCMT from *Candida* are listed in Table 5.

of methyl group donor AdoMet [64]. In another study by Lamarré and Desrosiers [65], it was demonstrated that incubating U-87 astrocytoma cells with mood stabilizing compound like lithium increases PCMT expression in those cells. LiCl is a Glycogen Synthase Kinase 3 or GSK-3 inhibitor that acts through stabilizing β-catenin that in turn plays important role in gene expression and cell proliferation [65]. Based on these findings, stationary phase *C. utilis* cells were incubated with increasing concentrations of AdOx and LiCl with an aim to alter CuPCMT levels *in vivo*. After 24 h incubation the PCMT activity in AdOx incubated cells were lower than control cells by 60% while that in LiCl incubated sets the activities had increased by 225% (Fig. 8A). ROS generation in the treated cells were measured as an indicator of any stress conditions they were generating. Incubation with increasing concentrations of AdOx led to production of ROS in cells but levels were lower when we compared the same with cells incubated in 0–2 mM LiCl (Fig. 8B and C). Increase of ROS concentration in AdOx incubated sets was gradual and at the concentration that induce maximum inhibition of CuPCMT activity, less than 20% of the cells were seen to generate ROS (Fig. 8B). In LiCl incubated sets, ROS generation was higher (Fig. 8C). Fanélus and Desrosiers [66] published that ROS formation enhanced PAO-mediated up-regulation of PCMT expression in U-87 human astroglioma cells. In a recent publication by Ouazia et al. [67], it was stated that in SH-SY5Y cells, overexpression of PCMT reduces cellular dopamine induced ROS levels along with rescue from apoptosis mediated cell death. Experiments with the *pcmt* deletion mutant revealed that indeed in cells devoid of CuPCMT activity, ROS levels upon incubation with LiCl was higher than in presence of increased CuPCMT activity (Fig. 8C). Semi-quantitative RT-PCR revealed that increasing concentrations of LiCl induces increased CuPCMT gene expression which may be the reason behind increased PCMT activity in *C. utilis* (Fig. 8D). AdOx incubated cells (0.8 mM) accumulated higher levels of isoAsp which might be attributed towards inhibition of PCMT activity (Fig. 8E). Conversely, in presence of LiCl isoAsp levels remained steady even under stress which might be attributed to the enhanced PCMT activity *in vivo* (Fig. 8F). Our study is the first to report the effect of LiCl on PCMT expression in unicellular yeasts like *C. utilis* thus elucidating the role of PCMT expression on survival of such unicellular yeasts.

The effects of *in vivo* regulation of CuPCMT activity levels were reflected in the ability of the *C. utilis* cells to withstand physiological stresses. Wild type *C. utilis* cells incubated with 1 mM LiCl and 0.8 mM AdOx for 24 h were subjected to physiological stress like oxidative, pH, hyperosmotic and heat. In AdOx treated sets where CuPCMT activity is inhibited, cells accumulated higher isoAsp moieties in cell lysates under stress conditions (Fig. 8E). Intracellular isoAsp levels were reduced when LiCl treated sets were subjected to physiological stress conditions (Fig. 8F). Correlation between increased intracellular isoAsp levels and reduced cell longevity was established when cell viability was assessed in treated sets subjected to physiological stress. Cell viability increased when cells treated with LiCl were subjected to stress in comparison with untreated sets under similar conditions (Fig. 9A, C, E and G). LiCl treatment also rescued cells from apoptotic or necrotic cell deaths (Fig. 9B, D, F and H). The key to this cell fate could be attributed to CuPCMT activity *in vivo* and it may be concluded that its protein repairing properties play an important role in maintaining cellular viability as well as to withstand physiological stress conditions in *C. utilis*.

Despite much information available regarding the action mechanism of PCMT and its role in extending cell longevity, workers have concentrated primarily on individual candidate proteins and peptide. Zhu et al. and Vigneswara et al., both in 2006, have conducted separate studies to identify the cellular targets of the enzyme in PCMT deficient rat and mouse brain respectively [6,68]. The on-blot methylation assay was aimed at radioactively labeling the specific isoaspartate moieties that formed in the absence of the repairing actions of the PCMT. Both studies identified neurologically important proteins as PCMT substrates and emphasized the enzyme's importance in maintaining normal neuronal function [6,68]. Neurones are highly specialized differentiated cells with a distinctive protein pool, unlike unicellular eukaryotes like yeasts that pack proteins associated with diverse but basic physiological functions in a single cell. Identification of the proteins susceptible to isoaspartate accumulation and methylation by PCMT can shed light on the physiological pathways affected by PCMT. *C. utilis* cells were incubated with 1 mM AdOx for 24 h to inhibit PCMT activity. The proteins that were normally repaired by PCMT will have a higher isoAsp level since the enzyme activity have been impaired. These isoAsp moieties would be methylated by external PCMT during the on-blot methylation assay and use of a radioactively labeled methyl group that will be incorporated in these isoAsp containing sites can be identified by X-ray radiography. These protein spots that appear in the autoradiograph are those proteins that contain the radioactively labelled methyl groups transferred to isoAsp containing proteins by externally added CuPCMT. The corresponding protein spots from the gel could be excised processed and could subsequently be identified by MS analysis (Fig. 10, Table 5). Since, the *C. utilis* genome has not yet been fully sequenced and annotated; the MALDI TOF MS/MS data were matched with yeast proteins to identify the closest homologs (Table 5). The cut-off peptide score was kept within 70. Only the peptides with the highest score of $\geq 70 \pm 2$ were recognised since they have the highest probability of being a homolog of the actual protein identified. The 29 homologous proteins identified were

found to be associated with important physiological pathways like metabolite synthesis, cell signalling, bio-molecule transport, stress response and even ribosome synthesis. Association of PCMT with these housekeeping metabolic processes rather than some very specific protein population indicate that in a unicellular eukaryote like *C. utilis*, protein repair by PCMT is crucial for maintaining cellular integrity. This result clearly points out the underlying reason for decreased cell survivability under stress when treated with AdOx (Fig. 9A–F).

From the last couple of decades, yeasts have been widely used for investigating many aspects of complex biological processes in eukaryotes owing to homology with those in mammalian system [69]. These unicellular organisms with their simple growth requirements, rapid cell division, ease of genetic manipulation and growing list of experimental tools for genome-wide analysis of biological functions, produce a lucrative platform for various applications such as establishing complex disease models and preliminary drug screening for the same [70,71]. More and more such yeasts are emerging as potential candidates with the growing wealth of whole genome sequence information. Since the most popular yeast *S. cerevisiae* lacks a PCMT gene homolog, its use to investigate complex role of the same in cellular signalling as well as its role in various diseases like cancer will be limited. Knowledge of the *C. utilis* genome sequence will facilitate genetic manipulations of this yeast to improve its future use for biotechnological applications in regard to further elucidating the cellular role of PCMT.

5. Conclusion

The aim of the study was to investigate a protein isoaspartyl methyltransferase enzyme from yeast where information is scarce on this topic. The study reports the identification and purification of an isoaspartyl methyltransferase in its native form from the yeast *C. utilis*. Elevated levels of the 25 kDa CuPCMT helps maintain cellular functions under stress by initiating repair of isoaspartyl moieties in proteins involved in all the major cellular processes.

Acknowledgments

Authors thank The Director, CSIR-IICB. Thanks are due to CSIR, New Delhi for providing Emeritus Fellowship Grant to AKG (Contract grant number: 21 (0855)/11/EMR-II) and Research Fellowship to SB, SL, TD.

Appendix A. Supplementary material

Supplementary data associated with this article can be found in the online version at http://dx.doi.org/10.1016/j.bbrep.2015.08.015.

References

[1] S. Clarke, A protein carboxyl methyltransfease that recognizes and repairs age-damaged peptides and proteins and participates in their repair, World Scientific Publishings, NJ, 1999.
[2] D.W. Aswad, M.V. Paranandi, B.T. Schurter, Isoaspartate in peptides and proteins: formation, significance, and analysis, J. Pharm. Biomed. Anal. 21 (2000) 1129–1136.
[3] T. Takata, J.T. Oxford, B. Demeler, K.J. Lampi, Deamidation destabilizes and triggers aggregation of a lens protein, βA3-crystallin, Protein Sci. 17 (2008) 1565–1575.
[4] J.D. Lowenson, S. Clarke, Structural elements affecting the recognition of L-isoaspartyl residues by the L-isoasparty/D-aspartyl protein methyltransferase. Implications for the repair hypothesis, J. Biol. Chem. 266 (1991) 19396–19406.
[5] T. Furuchi, K. Sakurako, M. Katane, M. Sekine, H. Homma, The role of protein L-Isoaspartyl/D-aspartyl O-methyltransferase (PIMT) in intracellular signal transduction, Chem Biodivers. 7 (2010) 1337–1348.
[6] J.X. Zhu, H.A. Doyle, M.J. Mamula, D.W. Aswad, Protein repair in the brain, proteomic analysis of endogenous substrates for Protein L-Isoaspartyl Methyltransferase in mouse brain, J. Biol. Chem. 281 (2006) 33802–33813.
[7] T. Dutta, S. Banerjee, D. Soren, S. Lahiri, S. Sengupta, J.A. Rasquinha, A.K. Ghosh, Regulation of enzymatic activity by deamidation and their subsequent repair by Protein L-isoaspartyl Methyl transferase, Appl. Biochem. Biotechnol. 168 (2012) 2358–2375.
[8] R.M. Kagan, H.J. McFadden, P.N. McFadden, C. O'Connor, S. Clarke, Molecular phylogenetics of a protein repair methyltransferase, Comp. Biochem. Physiol. 117B (1997) 379–385.
[9] C. Li, S. Clarke, Distribution of an L-isoaspartyl protein methyltransferase in eubacteria, J. Bacteriol. 174 (1992) 355–361.
[10] N. Thapar, A. Kim, S. Clarke, Distinct patterns of expression but similar biochemical properties of protein L-Isoaspartyl Methyltransferase in higher plants, Plant Physiol. 125 (2001) 1023–1035.
[11] R.M. Kagan, S. Clarke, Protein L-isoaspartyl methyltransferase from the nematode *Caenorhabditis elegans*: genomic structure and substrate specificity, Biochemistry 34 (1995) 10794–10806.
[12] M.B. O'Connor, A. Galus, M. Hartenstine, M. Magee, M.R. Jackson, C. M. O'Connor, Structural organization and developmental expression of the protein L-isoaspartyl methyltransferase gene from *Drosophila melanogaster*, Insect Biochem. Mol. Biol. 27 (1997) 49–54.
[13] J.M. Gilbert, A. Fowler, J. Bleibaum, S. Clarke, Purification of homologous protein carboxyl methyltransferase isozymes from human and bovine erythrocytes, Biochemistry 27 (1988) 5227–5233.
[14] T. Shimizu, T. Ikegami, M. Ogawara, Y. Suzuki, M. Takahashi, H. Morio, T. Shirasawa, Transgenic expression of the protein-L-isoaspartyl methyltransferase (PIMT) gene in the brain rescues mice from the fatal epilepsy of PIMT deficiency, J. Neurosci. Res. 69 (2002) 341–352.
[15] J. Kindrachuk, J. Parent, G.F. Davies, M. Dinsmore, S. Attah-Poku, S. Napper, Overexpression of L-isoaspartate O-methyltransferase in *Escherichia coli* increases heat shock survival by a mechanism independent of methyltransferase activity, J. Biol. Chem. 278 (2003) 50880–50886.
[16] S. Khare, C.L. Linster, S. Clarke, The interplay between protein l-isoaspartyl methyltransferase activity and insulin-like signaling to extend lifespan in *Caenorhabditis elegans*, PLoS ONE 6 (2011) e20850, http://dx.doi.org/10.1371/journal.pone.0020850.
[17] A. Goffeau, B.G. Barrell, H. Bussey, R.W. Davis, B. Dujon, H. Feldmann, F. Galibert, J.D. Hoheisel, C. Jacq, M. Johnston, E.J. Louis, H.W. Mewes, Y. Murakam,i, P. Philippsen, H. Tettelin, S.G. Oliver, Life with 6000 genes, Science 274 (1996) 546–567.
[18] A.N. Patananan, J. Capri, J.P. Whitelegge, S.G. Clarke, Non-repair pathways for minimizing protein isoaspartyl damage in the yeast *Saccharomyces cerevisiae*, J. Biol. Chem. 289 (2014) 16936–16953.
[19] A. Matsuyama, R. Arai, Y. Yashiroda, A. Shirai, A. Kamata, S. Sekido, Y. Kobayashi, A. Hashimoto, A. Hamamoto, Y. Hiraoka, S. Horinouchi, M. Yoshida, ORFeome cloning and global analysis of protein localization in the fission yeast *Schizosaccharomyces pombe*, Nat. Biotechnol. 24 (2006) 841–847.
[20] A. Roy, A.K. Ghosh, Correlation between stationary phase survival and acid trehalase activity in yeast, Biochim. Biophys. Acta 1401 (1998) 235–238.
[21] M.S. Longtine, A. McKenzie, D.J. Demarini, N.G. Shah, A. Wach, A. Bracha,t, P. Philippsen, J.R. Pringle, Additional modules for versatile and economical PCR-based gene deletion and modification in *Saccharomyces cerevisiae*, Yeast 14 (1998) 953–961.
[22] R.D. Gietz, R.A. Woods, Transformation of yeast by lithium acetate/single-stranded carrier DNA/polyethylene glycol method, Methods Enzymol. 350 (2002) 87–96.
[23] O.H. Lowry, N.J. Rosebrough, A.L. Farr, R. Randal, Protein measurement with the Folin phenol reagent, J. Biol. Chem. 193 (1951) 265–275.
[24] H.U. Bergmeyer, E. Brent, Aminotransferases, 2nd Ed., Academic Press. Inc., NY, 1974.
[25] M. Magnani, M. Dachà, V. Stocchi, P. Ninfali, G. Fornaini, Rabbit red blood cell hexokinase. Purification and properties, J. Biol. Chem. 255 (1980) 1752–1756.
[26] W. Lee, S. Shin, S.S. Cho, J. Park, Purification and characterization of glutamate dehydrogenase as another isoprotein binding to the membrane of rough endoplasmic reticulum, J. Cell. Biochem. 76 (1999) 244–253.
[27] U.K. Laemmli, Cleavage of structural proteins during the assembly of the head of bacteriophage T4, Nature 227 (1970) 680–685.
[28] M.A. Andrade, P. Chacón, J.J. Merelo, F. Morán, Evaluation of secondary structure of proteins from UV circular dichroism spectra using an unsupervised learning neural network, Protein Eng. 6 (1993) 383–390.
[29] I.H. Segel. Enzymes. In: Biochemical Calculations, John Wiley & Sons NY, 1976.
[30] M. Dixon, The graphical determination of K_m and K_i, Biochem. J. 129 (1972) 197–202.
[31] R.L. Gundry, M.Y. White, C.I. Murray, L.A. Kane, Q. Fu, B.A. Stanley, J.E. Van Eyk, Preparation of proteins and peptides for mass spectrometry analysis in a bottom-up proteomics workflow, Curr. Protoc. Mol. Biol. 88 (2009) 10.25.1–10.25.23.
[32] M. Goujon, H. McWilliam, W. Li, F. Valentin, S. Squizzato, J. Paern, R. Lopez, A new bioinformatics analysis tools framework at EMBL-EBI, Nucl. Acids Res. 38 (2010) W695–W699 , Suppl.
[33] S.F. Altschul, W. Gish, W. Miller, E.W. Myers, D.J. Lipman, Basic local alignment

search tool, J. Mol. Biol. 215 (1990) 403–410.
[34] H. Nordberg, M. Cantor, S. Dusheyko, S. Hua, A. Poliakov, I. Shabalov, T. Smirnova, I.V. Grigoriev, I. Dubchak, The genome portal of the department of energy joint genome institute: 2014 updates, Nucleic Acids Res. 42 (1) (2014) D26–D31.
[35] ⟨http://genome.jgi.doe.gov/pages/blast-query.jsf?db=Cybja1/23.11.2014⟩.
[36] Arnaud, M.B., Inglis, D.O., Skrzypek, M.S., Binkley, J., Shah, P., Wymore, F., Binkley, G., Miyasato, S. R, Simison, M., Sherlock, G. Candida Genome Database ⟨http://www.candidagenome.org/30.12.2014⟩.
[37] D.T. Jones, Protein secondary structure prediction based on position-specific scoring matrices, J. Mol. Biol. 292 (1999) 195–202.
[38] A. Marchler-Bauer, S. Lu, J.B. Anderson, F. Chitsaz, M.K. Derbyshire, C. DeWeese-Scott, J.H. Fong, L.Y. Geer, R.C. Geer, N.R. Gonzales, M. Gwadz, D. I. Hurwitz, J.D. Jackson, Z. Ke, C.J. Lanczycki, F. Lu, G.H. Marchler, M. Mullokandov, M.V. Omelchenko, C.L. Robertson, J.S. Song, N. Thanki, R. A. Yamashita, D. Zhang, N. Zhang, C. Zheng, S.H. Bryant, CDD: a conserved domain database for the functional annotation of proteins, Nucleic Acids Res. 39 (suppl 1) (2011) SD225–SD229.
[39] F. Sievers, A. Wilm, D. Dineen, T.J. Gibson, K. Karplus, W. Li, R. Lopez, H. McWilliam, M. Remmert, J. Söding, J.D. Thompson, D.G. Higgins, Fast, scalable generation of high-quality protein multiple sequence alignments using Clustal Omega, Mol. Syst. Biol. 7 (2011) 539.
[40] H. Zhang, S. Gao, M.J. Lercher, S. Hu, W. Chen, EvolView, an online tool for visualizing, annotating and managing phylogenetic trees, Nucleic Acids Res. 40 (W1) (2012) W569–W572.
[41] A. Kolkman, M.M.A. Olsthoorn, C.E.M. Heeremans, A.J.R. Heck, M. Slijper, Comparative proteome analysis of *Saccharomyces cerevisiae* grown in chemostat cultures limited for glucose or ethanol, Mol. Cell. Proteomics 4 (2005) 1–11.
[42] G.J. Morrison, R. Ganesan, Z. Qin, D.W. Aswad, Considerations in the Identification of Endogenous Substrates for Protein L-Isoaspartyl Methyltransferase: The Case of Synuclein, PLoS ONE (2012), http://dx.doi.org/10.1371/journal.pone.0043288.
[43] K. Kersters, G.L. Hemebert, R. De Wachter, Phylogenetic analysis of five medically important Candida species as deduced on the basis of small ribosomal subunit RNA sequences 7, Gen. Microbiol. 37 (1991) 1223–1230.
[44] M.-W. Chen, J. Anne, G. Volckaert, E. Huysmans, A. Vandenberghe, R. De Wachter, The nucleotide sequences of the 5 S rRNAs of seven molds and a yeast and their use in studying ascomycete phylogeny, Nudeic Adds. Res. 12 (1984) 4881–4892.
[45] A. Roetzer, T. Gabaldón, C. Schüller, From *Saccharomyces cerevisiae* to *Candida glabrata* in a few easy steps: important adaptations for an opportunistic pathogen, Fems Microbiol. Lett. 314 (1) (2011) 1–9, http://dx.doi.org/10.1111/j.1574-6968.2010.02102.x.
[46] S. Lahiri, A. Basu, S. Sengupta, S. Banerjee, T. Dutta, D. Soren, K. Chattopadhyay, A.K. Ghosh, Purification and characterization of a trehalase–invertase enzyme with dual activity from *Candida utilis*, Arch. Biochem. Biophys. 522 (2012) 90–99.
[47] S. Sengupta, S. Lahiri, S. Banerjee, B. Bashistha, A.K. Ghosh, Arginine mediated purification of trehalose-6-phosphate synthase (TPS) from *Candida utilis*: Its characterization and regulation, Biochim. Biophys. Acta 12 (2011) 1346–1354.
[48] H. Van Urk, P.R. Mark, W.A. Scheffers, J.P. Van Dijken, Metabolic responses of Saccharomyces *cerevisiae* CBS 8066 and *Candida utilis* CBS 621 upon transition from glucose limitation to glucose excess, Yeast 4 (1988) 283–291, http://dx.doi.org/10.1002/yea.320040406.
[49] E. Postma, A. Kuiper, W.F. Tomasouw, W.A. Scheffers, J.P. van Dijken, Competition for glucose between the yeasts Saccharomyces cerevisiae and *Candida utilis*, Appl. Env. Microbiol. *55* (12) (1989) 3214–3220.
[50] J.D. Lowenson, E. Kim, S.G. Young, S. Clarke, Limited accumulation of damaged proteins in L-isoaspartyl (D-aspartyl) *O*-methyltransferase-deficient mice, J. Biol. Chem. 276 (2001) 20695–20702.
[51] A. Niewmierzycka, S. Clarke, Do damaged proteins accumulate in *Caenorhabditis elegans* L-isoaspartate methyltransferase (pcm-1) deletion mutants? Arch. Biochem. Biophys. 364 (1999) 209–218.
[52] S. Dai, W. Ni, A.N. Patananan, S.G. Clarke, B.L. Karger, Z.S. Zhou, Integrated proteomic analysis of major isoaspartyl-containing proteinsin the urine of wild type and protein L-isoaspartate *O*-methyltransferase-deficient mice, Anal. Chem. 85 (2013) 2423–2430.
[53] A.R. Lajmi, S. Nochumson, Impact of antibody aggregation on a flow through anion-exchange membrane process, Biotechnol. Prog. 26 (2010) 1654–1661.
[54] N. Thapar, S. Clarke, Expression, purification, and characterization of the protein repair L-Isoaspartyl Methyltransferase from *Arabidopsis thaliana*, Protein Exp. Purif. 20 (2000) 237–251.
[55] C.L. David, D.W. Aswad, Cloning, Expression and Purification of Rat Brain Protein L-isoaspartyl Methyltransferase, Protein Exp. Purif. 6 (1995) 312–318.
[56] J.K. Ichikawa, S. Clarke, A highly active protein repair enzyme from an extreme thermophile: the L-isoaspartyl methyltransferase from *Thermotoga maritima*, Arch. Biochem. Biophys. 358 (1998) 222–231.
[57] N. Thapar, S.C. Griffith, T.O. Yeates, S. Clarke, Protein repair methyltransferase from the hyperthermophilic archaeon *Pyrococcus furiosus*: unusual methyl-accepting affinity for D-aspartyl and N-succinyl-containing peptides, J. Biol. Chem. 277 (2002) 1058–1065.
[58] P.I. Diaz, L.D. Strausbaugh, A. Dongari-Bagtzoglou, Fungal-bacterial interactions and their relevance to oral health: linking the clinic and the bench, Front. Cell. Infect. Microbiol. 4 (2014) 101, http://dx.doi.org/10.3389/fcimb.2014.00101.
[59] H. Ramshini, N. Rezaei-Ghaleh, A. Ebrahim-Habibi, A.A. Saboury, M. Nemat-Gorgani, Thermally induced changes in the structure and activity of yeast hexokinase *B*, Biophys. Chem. 137 (2–3) (2008) 88–94, http://dx.doi.org/10.1016/j.bpc.2008.07.004.
[60] F. Paradisi, J.L. Dean, K.F. Geoghegan, P.C. Engel, Spontaneous chemical reversion of an active site mutation: deamidation of an asparagine residue replacing thecatalytic aspartic acid of glutamate dehydrogenase, Biochemistry 44 (9) (2005) 3636–3643.
[61] S. Sinha, L. Zhang, S. Duan, T.D. Williams, J. Vlasak, R. Ionescu, E.M. Topp, Effect of protein structure on deamidation rate in the Fc fragment of an IgG1 monoclonal antibody, Protein Sci. 18 (8) (2009) 1573–1584, http://dx.doi.org/10.1002/pro.173.
[62] N.E. Robinson, A.B. Robinson, Prediction of protein deamidation rates from primary and three-dimensional structure, Proc. Natl. Acad. Sci. USA 98 (8) (2001) 4367–4372, http://dx.doi.org/10.1073/pnas.071066498.
[63] A.L. Young, W.G. Carter, H.A. Doyle, M.J. Mamula, D.W. Aswad, Structural integrity of histone H2B *in vivo* requires the activity of protein L-isoaspartyl methyltransferase, a putative protein repair enzyme, J. Biol. Chem. 276 (2001) 37161–37165.
[64] R.L. Bartel, R.T. Borchardt, Effects of adenosine dialdehyde on S-adenosylhomocysteine hydrolase and S-adenosylmethionine-dependent transmethylations in mouse L929 cells, Mol. Pharmacol. 25 (1984) 418–424.
[65] M. Lamarre, R.R. Desrosiers, Up-regulation of protein L-isoaspartyl methyltransferase expression by lithium is mediated by glycogen synthase kinase-3 inactivation and beta-catenin stabilization, Neuropharmacology 55 (5) (2008) 669–676.
[66] I. Fanélus, R.R. Desrosiers, Reactive oxygen species generated by thiol-modifying phenylarsine oxide stimulate the expression of protein L-isoaspartyl methyltransferase, Biochem. Biophys. Res. Commun. 371 (2008) 203–208.
[67] D. Ouazia, L.C. Levros Jr., É. Rassart, R.R. Desrosiers, The protein L-isoaspartyl (D-aspartyl) methyltransferase protects against dopamine-induced apoptosis in neuroblastoma SH-SY5Y cells, Neuroscience 295 (2015) 139–150.
[68] V. Vigneswara, J.D. Lowenson, C.D. Powell, M. Thakur, S. Clarke, D.E. Ray, W. G. Carter, Proteomic identification of novel substrates of a protein isoaspartyl methyltransferase repair enzyme, J. Biol. Chem. 281 (2006) 32619–32629.
[69] J.A. Simon, A. Bedalov, Yeast as a model system for anticancer drug discovery, Nat. Rev. Cancer 4 (2004) 481–487.
[70] A. Barrientos, Yeast models of human mitochondrial diseases, IUBMB Life 55 (2003) 83–95.
[71] L.H. Hartwell, P. Szankasi, C.J. Roberts, A.W. Murray, S.H. Friend, Integrating genetic approaches into the discovery of anticancer drugs, Science 278 (1997) 1064–1068.